Eur. Phys. J. C 48, 561–578 (2006)
DOI 10.1140/epjc/s10052-006-0076-7

THE EUROPEAN PHYSICAL JOURNAL C

Regular Article – Theoretical Physics

Energy and decay width of the πK atom

H. Jallouli[1,a], H. Sazdjian[2,b]

[1] Centre National des Sciences et Technologies Nucléaires, Technopole Sidi Thabet 2020, Tunisie
[2] Institut de Physique Nucléaire[c], Groupe de Physique Théorique, Université Paris XI, 91406 Orsay Cedex, France

Received: 26 May 2006 / Revised version: 13 July 2006 /
Published online: 27 October 2006 –

Abstract. The energy and the decay width of the πK atom are evaluated in the framework of the quasipotential-constraint theory approach. The main electromagnetic and isospin symmetry breaking corrections to the lowest-order formulas for the energy shift from the Coulomb binding energy and for the decay width are calculated. They are estimated to be of the order of a few per cent. We display formulas to extract the strong interaction S-wave πK scattering lengths from future experimental data concerning the πK atom.

PACS. 03.65.Pm; 11.10.St; 12.39.Fe; 13.40.Ks

1 Introduction

Hadronic atoms represent new tools for probing strong interaction dynamics at low energies [1–6]. If the hadronic constituents are pseudoscalar mesons, then the probe concerns the properties of spontaneous chiral symmetry breaking in QCD. The simplest representative in that case is the $\pi\pi$ atom (pionium), which was produced and studied in the DIRAC experiment at CERN [7, 8] and to which many theoretical studies were devoted [9–32]. At the next level in that category one finds the πK atom, the properties of which are tightly related to those of the $SU(3) \times SU(3)$ chiral symmetry breaking. In particular, the energies and widths of the atomic levels depend on the strong interaction πK scattering lengths and through them on various order parameters of chiral symmetry breaking. The theoretical interest of those quantities justifies the preparation of new experimental projects for the production and study of πK atoms [33, 34]. On theoretical grounds, the properties of the πK atom were recently studied in detail by Schweizer [35, 36] using the approach of nonrelativistic effective field theories to the bound state problem [37].

The present work is devoted to the study of the properties of the πK atom using the quasipotential-constraint theory approach [38–48] which was also applied to the pionium case [20–23] and which consists of a relativistic and covariant three-dimensional formulation of the bound state problem. Our aim is to calculate the $O(\alpha)$ corrections to the lowest-order formulas for the energy shift and decay width of the πK atom, where α is the fine structure constant, and to provide the means of extracting with sufficient precision the values of the strong interaction S-wave πK scattering lengths from future experimental data.

We introduce with respect to our previous approach to the pionium problem a slight modification, in that we formulate from the start the bound state problem almost on the mass shell. This is suggested by the substantial simplification one gains in order to reach the final results. The leading nonrelativistic formulas, which are of order α^3, are expressed mainly in terms of threshold properties of the strong interaction on-mass shell scattering amplitudes. In general, bound state problems in quantum field theories are formulated in terms of off-mass shell scattering amplitudes or kernels; on the other hand, effective lagrangians, like the one used in chiral perturbation theory, give rise to a proliferation of terms, some of which do not contribute on the mass shell. Therefore, one expects many cancellations among unphysical quantities, which are automatically realized in a formalism based from the start on the use of on-mass shell scattering amplitudes and their minimal analytic continuations.

However, because of the presence of infrared divergences, the on-mass shell formalism ceases to be consistent at higher orders in QED. Generally, up to $O(\alpha^4)$ effects in the bound state problem infrared divergences are unambiguously recognized, isolated and subtracted or cancelled, according to the method of approach. This is an implicit consequence of the Ward identities (and their analogues for mass terms) satisfied by the theory. At higher orders, for instance in the treatment of the Lamb shift problem, infrared divergences can no longer be isolated without ambiguity in an on-mass shell formalism of the bound state problem. The recourse to an off-mass shell formalism becomes compulsory at this stage [49–51]. For the present problem, since the precision that is sought does not neces-

[a] e-mail: hassen.jallouli@cnstn.rnrt.tn
[b] e-mail: sazdjian@ipno.in2p3.fr
[c] Unité Mixte de Recherche 8608 du CNRS, de l'IN2P3 et de l'Université Paris XI.

sitate the evaluation of $O(\alpha^5 \ln \alpha^{-1})$ effects, this difficulty will not show up.

The main corrections, of order α, to the lowest-order formulas can be represented by three groups of terms:

(i) the pure elecromagnetic corrections, arising beyond the Coulomb potential;
(ii) electromagnetic radiative corrections to the strong interaction scattering amplitudes, including isospin symmetry breaking effects;
(iii) second-order perturbation theory effects in the perturbative expansion of the bound state energy.

The sum of those corrections is found to be of the order of a few per cent relative to the leading terms. Our results agree with those obtained by Schweizer [35, 36].

The plan of the paper is the following. In Sect. 2, we present the general bound state formalism that we use. In Sect. 3, we consider the specific case of the πK atom, for which we adopt a coupled channel formalism. In Sect. 4, we calculate the lowest-order contributions to the real and imaginary parts of the energy shift. In Sect. 5, pure QED type corrections are evaluated. In Sect. 6, electromagnetic radiative corrections to the strong interaction scattering amplitudes are taken into account. In Sect. 7, a general property of cancellation of divergences of three-dimensional integrals, present in our formalism, is displayed. Section 8 deals with second-order effects of the perturbation theory expansion of the bound state energy. A summary of the results follows in Sect. 9. Some evaluations of integrals are presented in the appendix.

2 Bound state formalism

It is generally recognized, on the basis of the hamiltonian formalism, that relative times and relative energies of particles of multiparticle systems should not play a dynamical role in relativistic theories. Constraint theory [52–64] allows, through the use of first-class constraints, for the elimination of redundant variables, respecting at the same time the symmetries of the theory (in the present case Poincaré invariance). For a two-particle system, described by momenta p_1 and p_2, with physical masses m_1 and m_2, the following constraint eliminates the relative energy in a covariant way:

$$C(P,p) \equiv \left(p_1^2 - p_2^2\right) - \left(m_1^2 - m_2^2\right) = 0\,,$$
$$P = p_1 + p_2, \quad p = \frac{1}{2}\left(p_1 - p_2\right)\,. \tag{1}$$

That constraint also respects the symmetry between the two particles and remains valid on the mass shell or in the free case.

We next consider a prototype quantum field theory with a given lagrangian describing, among others, the interaction between two spin-0 particles, labeled 1 and 2. Let T be the on-mass shell elastic scattering amplitude of the process $1+2 \to 1'+2'$. [T is defined from the S matrix by the relation $S_{fi} = \delta_{fi} + (2\pi)^4 \delta^4(P - P')T_{fi}$, where P and P' are the total momenta of the ingoing and outgoing particles.] T is then a function of the two Mandelstam variables $s = P^2$ and $t = q^2$, with $q = (p_1 - p_1')$. For convenience, we define a modified scattering amplitude $\widetilde{T}$:

$$\widetilde{T}(s,t) = \frac{\mathrm{i}}{2\sqrt{s}} T(s,t)\,. \tag{2}$$

Since the equations we are developing are manifestly covariant, the total momentum P of the system defines a privileged direction and all momenta can be decomposed along longitudinal (one-dimensional) and transverse (three-dimensional) components with respect to P. However, to simplify notation, we shall henceforth stick to the center-of-mass frame ($\mathbf{P} = \mathbf{0}$) and represent vectors with their temporal and spatial components.

The starting point of the present formalism is the postulate that $\widetilde{T}$ satisfies, by means of an effective propagator g_0, a three-dimensional Lippmann–Schwinger type equation leading to the definition of a kernel or a potential $V(s,t)$:

$$V = \widetilde{T} - V\, g_0\, \widetilde{T}\,. \tag{3}$$

This equation can be used to calculate V either iteratively from $\widetilde{T}$, or from a perturbative expansion of $\widetilde{T}$ itself. The iterative integration is three-dimensional, taking into account constraint (1). Thus, if the two particle momenta linking $\widetilde{T}$ to V are $(p_1 - k)$ and $(p_2 + k)$, total momentum being conserved, constraint (1) applied to them yields $k_0 = 0$ and integration concerns the three-momentum $\mathbf{k}$. The latter integration does not, however, preserve the mass-shell character of $\widetilde{T}$; it forces the corresponding momentum transfer $-\mathbf{k}^2$ to take unphysical values down to $-\infty$. The situation here is very analogous to that of nonrelativistic dynamics. We consider it as corresponding to a minimal extension of the scattering amplitude to the off-shell case, in the sense that it does not imply introduction of new terms but simply an extension of the domain of validity of the expression of $\widetilde{T}$ to a larger one.

The expression of g_0 is chosen so that V is hermitian in the elastic unitarity region [45, 46]. Noticing that constraint (1) implies equality of the Klein–Gordon operators of particles 1 and 2,

$$H_0(s,\mathbf{p}) \equiv \left(p_1^2 - m_1^2\right)\big|_C = \left(p_2^2 - m_2^2\right)\big|_C = b_0^2(s) - \mathbf{p}^2,$$
$$b_0^2(s) \equiv \frac{s}{4} - \frac{1}{2}\left(m_1^2 + m_2^2\right) + \frac{\left(m_1^2 - m_2^2\right)^2}{4s}\,, \tag{4}$$

g_0 is chosen as the propagator associated with these operators:

$$g_0(s,\mathbf{p}) = \frac{1}{H_0(s,\mathbf{p}) + \mathrm{i}\varepsilon} = \frac{1}{b_0^2(s) - \mathbf{p}^2 + \mathrm{i}\varepsilon}\,. \tag{5}$$

On the mass shell, one has $\mathbf{p}^2 = b_0^2(s)$ and H_0 vanishes. However, inside the integration domain of the iterative series, $\mathbf{p}$ is replaced by $(\mathbf{p} - \mathbf{k})$ and H_0 takes the value $(2\mathbf{p}\cdot\mathbf{k} - \mathbf{k}^2)$.

It is advantageous in some instances to rewrite the scattering amplitude in terms of a two-particle irreducible

kernel. Introducing the two-particle irreducible kernel K and the two-particle free propagator G_0, one has $T = K + KG_0T$, and $\widetilde{T}$ takes the form

$$\widetilde{T} = \widetilde{K} + \widetilde{K}\,\widetilde{G}_0\,\widetilde{T}, \tag{6}$$

where $\widetilde{K} = iK/(2\sqrt{s}\,)$ and $\widetilde{G}_0 = -\mathrm{i}2\sqrt{s}G_0$, with

$$G_0 = G_{10}\,G_{20}, \quad G_{a0} = \frac{\mathrm{i}}{p_a^2 - m_a^2 + \mathrm{i}\varepsilon}, \quad a = 1,2\,. \tag{7}$$

Then the potential V can be expressed in terms of the kernel $\widetilde{K}$:

$$V = \widetilde{K}\left(1 - \left(\widetilde{G}_0 - g_0\right)\widetilde{K}\right)^{-1}, \tag{8}$$

the integrations involving $\widetilde{G}_0$ being four-dimensional.

We assume that V has been calculated (exactly or approximately) from $\widetilde{T}$ or $\widetilde{K}$. Because of the mass shell condition imposed on the external particles, it is, like $\widetilde{T}$, a function of s and t only: $V = V(s,t)$. In $\mathbf{x}$-space, obtained by Fourier transformation with respect to $\mathbf{q}\ (= (\mathbf{p} - \mathbf{p}'))$, it is a local function of $\mathbf{x}$; all the nonlocal character of the interaction is now contained in the energy dependence of V. That feature does not remain true in an off-mass shell formulation, where V may depend on the operator $\mathbf{p}^2$.

We next introduce the Green function associated with V and $\widetilde{T}$ (integrations on internal variables are implicit):

$$\begin{aligned} G(s;\mathbf{p},\mathbf{p}') &= (2\pi)^3\delta^3(\mathbf{p}-\mathbf{p}')g_0(s,\mathbf{p}) \\ &\quad + g_0(s,\mathbf{p})\,V(s,-\mathbf{k}^2)\,G(s;\mathbf{p}-\mathbf{k},\mathbf{p}') \\ &= g_0 + g_0\,\widetilde{T}\,g_0\,. \end{aligned} \tag{9}$$

Since G is an off-mass shell quantity, the external momenta $\mathbf{p}$ and $\mathbf{p}'$ are not restricted in the above equations to the mass shell and $\widetilde{T}$ is extended off the mass shell through the continuation of the variable t.

In the presence of bound states, G develops poles in s. (We assume C, P and T invariances.) Let s_0 be the mass squared of such a bound state ($s_0 > 0$); then, in the vicinity of s_0, G behaves as:

$$G \underset{s\to s_0}{\simeq} \frac{\Psi\,\Psi^\dagger}{(s - s_0 + \mathrm{i}\varepsilon)}\,, \tag{10}$$

where $\Psi^\dagger$ is the adjoint of Ψ. Since (by construction) the kernel V does not have singularities, at least in the vicinity of the two-body threshold, one deduces from (9) and (10) the wave equation

$$\left[\,g_0^{-1} - V\,\right]\Psi = 0\,. \tag{11}$$

The normalization and orthogonality properties of wave functions are obtained in the standard way [44, 47, 65]. Let us assume that the spectrum contains several nondegenerate bound states, labelled by an integer n, with masses squared $s_n > 0$. (Generalization to the degenerate case is straightforward.) Designating by G^{-1} the inverse of G $[G^{-1} = g_0^{-1} - V]$ and writing the wave equation of the bound state n as $G^{-1}(s_n)\Psi_{\mathrm{n}} = 0$, one easily arrives at the equation

$$\Psi_{\mathrm{n}}^\dagger\left(\frac{G^{-1}(s) - G^{-1}(s_n)}{s - s_n}\right)G(s) = \frac{\Psi_{\mathrm{n}}^\dagger}{s - s_n}\,. \tag{12}$$

Taking successively the limits $s \to s_n$ and $s \to s_m$ $(m \neq n)$, one obtains the normalization and orthogonality conditions:

$$\int \frac{\mathrm{d}^3p}{(2\pi)^3}\,\Psi_{\mathrm{n}}^\dagger\left(\frac{\partial G^{-1}(s)}{\partial s}\right)\Big|_{s=s_n}\Psi_{\mathrm{n}} = 1\,, \tag{13}$$

$$\int \frac{\mathrm{d}^3p}{(2\pi)^3}\Psi_{\mathrm{n}}^\dagger\left(\frac{G^{-1}(s_n) - G^{-1}(s_m)}{s_n - s_m}\right)\Psi_m = 0, \quad s_n \neq s_m\,. \tag{14}$$

The perturbative calculation of energy shifts from a zeroth-order approximation is also obtained with standard techniques [28–30, 47, 65]. Let us assume that the kernel V can be separated into two parts,

$$V = V_1 + V_2\,, \tag{15}$$

such that the solutions corresponding to V_1 are known. Let G_1 be the Green function associated with V_1:

$$G_1 = g_0 + g_0\,V_1\,G_1\,. \tag{16}$$

We designate by φ_n the corresponding bound state wave functions with masses squared $s_n^{(0)}$. The complete Green function is constructed from G_1 and the kernel V_2:

$$G = G_1 + G_1V_2G\,. \tag{17}$$

The scattering amplitude due to V_2 is obtained from V_2 and G_1:

$$\widetilde{T}_2 = V_2 + V_2\,G_1\,\widetilde{T}_2\,, \tag{18}$$

from which one deduces:

$$G = G_1 + G_1\,\widetilde{T}_2\,G_1\,. \tag{19}$$

To obtain the perturbative expansion around the bound state n, one isolates the corresponding pole in G_1:

$$G_1 = G_1' + \frac{\varphi_n\varphi_n^\dagger}{\left(s - s_n^{(0)} + \mathrm{i}\varepsilon\right)}\,. \tag{20}$$

The reduced scattering amplitude $\widetilde{T}_2'$ is constructed from the reduced Green function G_1' and V_2:

$$\widetilde{T}_2' = V_2 + V_2\,G_1'\,\widetilde{T}_2'\,. \tag{21}$$

The relationship between $\widetilde{T}_2$ and $\widetilde{T}_2'$ is:

$$\widetilde{T}_2 = \left(1 - \widetilde{T}_2'\,\frac{\varphi_n\varphi_n^\dagger}{\left(s - s_n^{(0)} + \mathrm{i}\varepsilon\right)}\right)^{-1}\widetilde{T}_2'\,. \tag{22}$$

Expressing in (19) G_1 and $\widetilde{T}_2$ in terms of G_1', $\widetilde{T}_2'$ and the pole term, one obtains the decomposition (integrations are implicit)

$$G = G_1' + G_1' \widetilde{T}_2' G_1' + \left(1 + G_1' \widetilde{T}_2'\right) \frac{\varphi_n \varphi_n^\dagger}{\left(s - s_n^{(0)} - \left(\varphi_n^\dagger \widetilde{T}_2' \varphi_n\right) + \mathrm{i}\varepsilon\right)} \left(1 + \widetilde{T}_2' G_1'\right), \tag{23}$$

from which one deduces the value of the mass squared of the bound state n [28–30]:

$$s_n = s_n^{(0)} + \left(\varphi_n^\dagger \widetilde{T}_2' \varphi_n\right). \tag{24}$$

Expansion of $\widetilde{T}_2'$ in terms of V_2 and G_1' according to (21) yields the perturbative series of s_n. Up to second order in V_2, the expression of s_n is [47, 65]

$$s_n = s_n^{(0)} + \Big\{ \left(\varphi_n^\dagger V_2 \varphi_n\right) + \left(\varphi_n^\dagger V_2 G_1' V_2 \varphi_n\right) + \left(\varphi_n^\dagger V_2 \varphi_n\right) \left(\varphi_n^\dagger \frac{\partial V_2}{\partial s} \varphi_n\right) \Big\}\Big|_{s=s_n^{(0)}}. \tag{25}$$

3 πK system

The πK atom is formed in the charged sector ($\pi^- K^+$ or its charge conjugate) under the effect of the Coulomb interaction and decays under the effect of the strong interaction predominantly into the neutral sector ($\pi^0 K^0$ or its charge conjugate). Branching ratios of other decays, involving photons, do not exceed a fraction of a per cent. It is natural to treat the πK system by means of a coupled channel formalism by generalizing the formalism developed in Sect. 2 with a matrix notation.

We label with the index c the quantities related to the charged sector ($\pi^- K^+$) and with the index n those related to the neutral sector ($\pi^0 K^0$). Because of the decay process $\pi^- K^+ \to \pi^0 K^0$, the energy of the bound state becomes complex with a negative imaginary part. The scattering amplitudes and Green functions involving the above sectors have a common pole at the position of the complex energy of the bound state. We introduce a two-component wave function Ψ by

$$\Psi = \begin{pmatrix} \Psi_\mathrm{c} \\ \Psi_\mathrm{n} \end{pmatrix} \tag{26}$$

and define the potential V in matrix form in the corresponding space:

$$V = \begin{pmatrix} V_\mathrm{cc} & V_\mathrm{cn} \\ V_\mathrm{nc} & V_\mathrm{nn} \end{pmatrix}. \tag{27}$$

The iteration effective propagator g_0 [see (3)–(5)] is now composed of two propagators:

$$g_0 = \begin{pmatrix} g_{0\mathrm{c}} & 0 \\ 0 & g_{0\mathrm{n}} \end{pmatrix}, \quad g_0^{-1} = \begin{pmatrix} g_{0\mathrm{c}}^{-1} & 0 \\ 0 & g_{0\mathrm{n}}^{-1} \end{pmatrix}. \tag{28}$$

$g_{0\mathrm{c}}$ and $g_{0\mathrm{n}}$ are defined with the physical masses of the particles, with respective energy factors $b_{0\mathrm{c}}^2(s)$ and $b_{0\mathrm{n}}^2(s)$ [see (4)].

The wave equation (11) takes now the form of two coupled equations:

$$\left(g_{0\mathrm{c}}^{-1} - V_\mathrm{cc}\right)\Psi_\mathrm{c} - V_\mathrm{cn}\Psi_\mathrm{n} = 0\,, \tag{29}$$

$$-V_\mathrm{nc}\Psi_\mathrm{c} + \left(g_{0\mathrm{n}}^{-1} - V_\mathrm{nn}\right)\Psi_\mathrm{n} = 0\,. \tag{30}$$

The wave function Ψ_n represents an outgoing wave created by the charged state; it can be eliminated in favor of Ψ_c, yielding the wave equation for the latter wave function:

$$g_{0\mathrm{c}}^{-1}\Psi_\mathrm{c} = V_\mathrm{cc}\Psi_\mathrm{c} + V_\mathrm{cn}\left(1 - g_{0\mathrm{n}}V_\mathrm{nn}\right)^{-1} g_{0\mathrm{n}}V_\mathrm{nc}\Psi_\mathrm{c}\,. \tag{31}$$

This is the bound state equation describing the properties of the πK atom.

The potentials V are calculated from the Lippmann–Schwinger type equation (3), written now in matrix form in terms of the scattering amplitudes of the processes $\pi^- K^+ \to \pi^- K^+$, $\pi^- K^+ \to \pi^0 K^0$, $\pi^0 K^0 \to \pi^- K^+$, $\pi^0 K^0 \to \pi^0 K^0$, which we designate respectively by $\widetilde{T}_\mathrm{cc}$, $\widetilde{T}_\mathrm{nc}$, $\widetilde{T}_\mathrm{cn}$ and $\widetilde{T}_\mathrm{nn}$, $\widetilde{T}$ being defined in (2). The relationships of the components of V and $\widetilde{T}$ are

$$\begin{aligned} V_\mathrm{cc} &= \widetilde{T}_\mathrm{cc} - V_\mathrm{cc}\, g_{0\mathrm{c}}\, \widetilde{T}_\mathrm{cc} - V_\mathrm{cn}\, g_{0\mathrm{n}}\, \widetilde{T}_\mathrm{nc}\,, \\ V_\mathrm{cn} &= \widetilde{T}_\mathrm{cn} - V_\mathrm{cc}\, g_{0\mathrm{c}}\, \widetilde{T}_\mathrm{cn} - V_\mathrm{cn}\, g_{0\mathrm{n}}\, \widetilde{T}_\mathrm{nn}\,, \\ V_\mathrm{nc} &= \widetilde{T}_\mathrm{nc} - V_\mathrm{nc}\, g_{0\mathrm{c}}\, \widetilde{T}_\mathrm{cc} - V_\mathrm{nn}\, g_{0\mathrm{n}}\, \widetilde{T}_\mathrm{nc}\,, \\ V_\mathrm{nn} &= \widetilde{T}_\mathrm{nn} - V_\mathrm{nc}\, g_{0\mathrm{c}}\, \widetilde{T}_\mathrm{cn} - V_\mathrm{nn}\, g_{0\mathrm{n}}\, \widetilde{T}_\mathrm{nn}\,. \end{aligned} \tag{32}$$

When electromagnetism and isospin symmetry breaking are switched off, one remains with the strong interaction or hadronic amplitudes $\widetilde{T}_h$ in the isospin symmetry limit; these are related to the isospin invariant amplitudes $\widetilde{T}^I$ in the following way:

$$\begin{aligned} \widetilde{T}_{\mathrm{cc},h} &= \frac{1}{3}\left(2\widetilde{T}^{1/2} + \widetilde{T}^{3/2}\right), \\ \widetilde{T}_{\mathrm{cn},h} &= \widetilde{T}_{\mathrm{nc},h} = -\frac{\sqrt{2}}{3}\left(\widetilde{T}^{1/2} - \widetilde{T}^{3/2}\right), \\ \widetilde{T}_{\mathrm{nn},h} &= \frac{1}{3}\left(\widetilde{T}^{1/2} + 2\widetilde{T}^{3/2}\right). \end{aligned} \tag{33}$$

One also defines the isospin even (+) and odd (−) amplitudes:

$$\begin{aligned} \widetilde{T}^+ &= \frac{1}{3}\left(\widetilde{T}^{1/2} + 2\widetilde{T}^{3/2}\right), \\ \widetilde{T}^- &= \frac{1}{3}\left(\widetilde{T}^{1/2} - \widetilde{T}^{3/2}\right). \end{aligned} \tag{34}$$

The decomposition into partial waves is done according to the formula (in the c.m. frame)

$$-2\sqrt{s}\,\widetilde{T}^I(s,t) = 16\pi \sum_{\ell=0}^{\infty} (2\ell+1) t_\ell^I(s) P_\ell(\cos\theta)\,, \tag{35}$$

while the scattering lengths and effective ranges are defined from the threshold expansion of the real part of t_ℓ^I:

$$\mathcal{R}e\, t_\ell^I(s) = \frac{\sqrt{s}}{2}\left(\mathbf{p}^2\right)^\ell \left(a_\ell^I + b_\ell^I \mathbf{p}^2 + O\left(\left(\mathbf{p}^2\right)^2\right)\right). \quad (36)$$

The iteration series (32) defining the potentials involve with the presence of the effective propagators g_0 three-dimensional diagrams, which we call *constraint diagrams* due to the constraint (1) that is used there (see Sect. 2). They cancel the s-channel singularities of the scattering amplitudes in the scattering region and provide potentials that are real and regular in the total energy variable, being thus appropriate for a continuation to the bound state region.

For Feynman diagrams involving QED parts, the calculation of V can be done with a simultaneous perturbative expansion of the scattering amplitude in the fine structure constant α. Since the bound state region is close to the two-particle threshold, one can use for the evaluation of the magnitude of the corresponding terms the threshold expansion method developed by Beneke and Smirnov [66], which consists of making the expansion already at the level of the integrand, using dimensional regularization, by recognizing the various types of infrared singularities that might arise. The momenta that are relevant for that type of analysis are classified as potential, soft, ultrasoft and hard [66].

In order to apply perturbation theory to (31) for the evaluation of the bound state energy levels, it is natural to choose the nonrelativistic Coulomb potential as the zeroth-order potential, associated with the nonrelativistic kinetic energy. To this end, we separate from the total energy P_0 the mass term by defining (in the c.m. frame) the binding energy $\mathcal{E}$:

$$\sqrt{s} = P_0 = m_{\pi^-} + m_{K^+} + \mathcal{E}\,. \quad (37)$$

Expanding s with respect to $\mathcal{E}$, one has for the c.m. momentum squared factor $b_{0\mathrm{c}}^2(s)$ [see (4)]

$$b_{0\mathrm{c}}^2(s) \simeq 2\mu\mathcal{E}\left(1 + \left(\frac{m_{\pi^-}^2 + m_{K^+}^2 - m_{\pi^-}m_{K^+}}{2m_{\pi^-}m_{K^+}\left(m_{\pi^-}+m_{K^+}\right)}\right)\mathcal{E}\right),$$
$$\mu = \frac{m_{\pi^-}m_{K^+}}{\left(m_{\pi^-}+m_{K^+}\right)}\,. \quad (38)$$

The Coulomb potential, which we designate by V_{C}, appears in the nonrelativistic expansion of the potential V_{cc} with the coefficient 2μ:

$$V_{\mathrm{cc}} = 2\mu V_{\mathrm{C}} + \overline{V}_{\mathrm{cc}}\,, \qquad V_{\mathrm{C}} = -\frac{\alpha}{r}\,. \quad (39)$$

Therefore, we can divide the whole wave equation by 2μ and recover at zeroth order the nonrelativistic hamiltonian. The quadratic part in $\mathcal{E}$ in the expression of $b_0^2(s)$ above can then be treated as a part of the perturbation. Furthermore, by absorbing in the definition of wave functions the factor $(\mu/(m_{\pi^-}+m_{K^+}))^{1/2}$ (within the present approximation) one recovers from (13) the usual nonrelativistic normalization for the zeroth-order wave functions φ_n:

$$\int \frac{\mathrm{d}^3p}{(2\pi)^3}\varphi_n^\dagger\varphi_n = 1\,. \quad (40)$$

Thus, φ satisfies the Schrödinger equation

$$E_n^{(0)}\,\varphi_{n\ell}^m = \left(\frac{\mathbf{p}^2}{2\mu} + V_{\mathrm{C}}\right)\varphi_{n\ell}^m\,, \quad E_n^{(0)} = -\frac{\mu\alpha^2}{2n^2}\,,$$
$$n \geq \ell + 1\,, \quad (41)$$

with n, ℓ and m representing the principal, orbital and azimuthal quantum numbers, respectively.

Similarly, isolating, as in (37), from the bound state energies the mass term, by writing $\sqrt{s_n} = m_{\pi^-} + m_{K^+} + \mathcal{E}_n$ and $\sqrt{s_n^{(0)}} = m_{\pi^-} + m_{K^+} + E_n^{(0)}$, we recover from (25) the perturbation series of the nonrelativistic theory, written here up to second order:

$$\mathcal{E}_n = E_n^{(0)} + \left(\frac{1}{2\mu}\right)\left\{\left(\varphi_n^\dagger V_2 \varphi_n\right) + \left(\varphi_n^\dagger V_2 G_1' V_2\,\varphi_n\right)\right\}\Big|_{\mathcal{E}=E_n^{(0)}}$$
$$- \left(\frac{m_{\pi^-}^2 + m_{K^+}^2 - m_{\pi^-}m_{K^+}}{2m_{\pi^-}m_{K^+}\left(m_{\pi^-}+m_{K^+}\right)}\right)E_n^{(0)2}\,. \quad (42)$$

The last term comes from the relativistic corrections of the left-hand side of the wave equation (31) (cf. (38)). The last term of (25) has been discarded, since it does not contribute to order α^4.

The bound state energy $\mathcal{E}_n$ is in general complex. We designate by E_n its real part; its imaginary part is equal to $-\Gamma_n/2$, where Γ_n is the decay width of the bound state into two neutral mesons. We thus have

$$\mathcal{E}_n = E_n - \frac{\mathrm{i}}{2}\Gamma_n\,. \quad (43)$$

The Green function G_1 [see (16)] that is associated with the zeroth-order potential V_1, is now essentially the Green function of the Coulomb potential, which we designate by G_{C}, the expression of which has been given by Schwinger [67]:

$$G_{\mathrm{C}}\left(E,\mathbf{p},\mathbf{p}'\right) = 2\mu G_1 = \frac{(2\pi)^3\delta^3\left(\mathbf{p}-\mathbf{p}'\right)}{\left(E-\mathbf{p}^2/(2\mu)\right)}$$
$$- \frac{1}{\left(E-\mathbf{p}^2/(2\mu)\right)}\,\frac{4\pi\alpha}{\left(\mathbf{p}-\mathbf{p}'\right)^2}\,\frac{1}{\left(E-\mathbf{p}'^2/(2\mu)\right)}$$
$$- \frac{1}{\left(E-\mathbf{p}^2/(2\mu)\right)}\,4\pi\alpha\eta I\left(E,\mathbf{p},\mathbf{p}'\right)\times\frac{1}{\left(E-\mathbf{p}'^2/(2\mu)\right)}$$
$$\simeq 2\mu\left\{g_{0\mathrm{c}} + g_{0\mathrm{c}}2\mu V_{\mathrm{C}} g_{0\mathrm{c}} - g_{0\mathrm{c}}8\pi\mu\alpha\eta I g_{0\mathrm{c}}\right\}, \quad (44)$$

where I and η are defined as

$$I(E,\mathbf{p},\mathbf{p}') = \int_0^1 \mathrm{d}\rho\,\rho^{-\eta}\left[\rho(\mathbf{p}-\mathbf{p}')^2\right.$$
$$\left. + (1-\rho)^2\frac{\eta^2}{\alpha^2}\left(E-\mathbf{p}^2/(2\mu)\right)\left(E-\mathbf{p}'^2/(2\mu)\right)\right]^{-1},$$
$$\eta = \frac{\alpha}{2\sqrt{-E/(2\mu)}}\,. \quad (45)$$

The quantity $G'_{\rm C}$ will then correspond to $G_{\rm C}$ from which the pole term around which perturbative expansion is organized is removed: $G'_{\rm C} = 2\mu G'_1$ [see (20)].

The potential V_2 that appears in the perturbative formula (42) is obtained from the wave equation (31), by subtracting from the kernel of the right-hand side the Coulomb part [see (39)]:

$$V_2 = \overline{V}_{\rm cc} + V_{\rm cn}\Big(1 - g_{0\rm n}V_{\rm nn}\Big)^{-1} g_{0\rm n}V_{\rm nc}\,. \tag{46}$$

In order to use this expression in (42), we first expand the factor $(1-g_{0\rm n}V_{\rm nn})^{-1}$ in $g_{0\rm n}$ and evaluate the order of magnitude of each term of the expansion. The integration of $g_{0\rm n}$ yields the factor $-{\rm i}\sqrt{b^2_{0\rm n}(s)}/(4\pi)$ [see (A.5)], where the total energy is fixed at the bound state energy and $b^2_{0\rm n}(s)$ is defined in (4) with masses of the neutral mesons, m_{π^0} and m_{K^0}; it is equal to the square of the c.m. momentum, which we represent by p^*, of the system $\pi^0 K^0$ after the decay of the bound state: $b^2_{0\rm n}(s) = p^{*2}$. The latter is essentially determined by the mass differences between charged and neutral mesons. Defining Δm as

$$2\Delta m \equiv m_{K^+} - m_{K^0} + m_{\pi^-} - m_{\pi^0} = 0.622\,{\rm MeV}, \tag{47}$$

one has approximately

$$\Big(\frac{p^*}{2\mu}\Big)^2 \simeq \frac{\Delta m}{\mu} \simeq 0.0029, \tag{48}$$

which is a quantity of the order of $\alpha/2$. Therefore, each $g_{0\rm n}$ can be estimated numerically as a quantity of the order of $\alpha^{1/2}$. Furthermore, the real part of the energy of the bound state receives contributions from even powers of $g_{0\rm n}$, while the imaginary part (the decay width) receives contributions from odd powers of $g_{0\rm n}$. With these estimates, (42) becomes:

$$\begin{aligned}
&2\mu\Delta\mathcal{E}_n = \\
&\Big\{\varphi^\dagger_{n\ell}\overline{V}_{\rm cc}\varphi_{n\ell} + \varphi^\dagger_{n\ell}V_{\rm cn}g_{0\rm n}V_{\rm nc}\varphi_{n\ell} + \varphi^\dagger_{n\ell}\overline{V}_{\rm cc}\frac{G'_{\rm C}}{2\mu}\overline{V}_{\rm cc}\varphi_{n\ell} \\
&+ \varphi^\dagger_{n\ell}\Big(\overline{V}_{\rm cc}\frac{G'_{\rm C}}{2\mu}V_{\rm cn}g_{0\rm n}V_{\rm nc} + V_{\rm cn}g_{0\rm n}V_{\rm nc}\frac{G'_{\rm C}}{2\mu}\overline{V}_{\rm cc}\Big)\varphi_{n\ell}\Big\}\Big|_{\mathcal{E}=E^{(0)}_n} \\
&- \left(\frac{m^2_{\pi^-} + m^2_{K^+} - m_{\pi^-}m_{K^+}}{(m_{\pi^-}+m_{K^+})^2}\right) E^{(0)2}_n\,.
\end{aligned} \tag{49}$$

Here, $\Delta\mathcal{E}_n$ represents the energy shift with respect to the nonrelativistic Coulomb bound state energy (41). We have retained, for the real part of the energy, terms contributing to the orders α^3 and α^4, while for the imaginary part of the energy (the decay width), we have retained terms contributing to the orders $\alpha^3(\Delta m/\mu)^{1/2}$ and $\alpha^4(\Delta m/\mu)^{1/2}$. Higher-order terms are numerically negligible.

4 Energy shift and decay width in lowest order

We evaluate in this section the lowest-order contributions, $O(\alpha^3)$ and $O(\alpha^3(\Delta m/\mu)^{1/2})$, to the real and imaginary parts of the energy, respectively; these come from the first two terms of the decomposition (49). Pure electromagnetic interactions beyond the Coulomb potential contribute only at $O(\alpha^4)$ and hence can be ignored at the present level. A similar conclusion holds also for the interference terms between strong and electromagnetic interactions. Therefore, one has to consider in the potentials $\overline{V}_{\rm cc}$, $V_{\rm cn}$ and $V_{\rm nc}$ solely contributions coming from strong interactions.

All qualitative properties that are derived subsequently depend only on the short-range nature of the strong interaction, or equivalently, on the absence of massless particles in it; the particular model used for representing the strong interaction scattering amplitude is not relevant, although we will particularly refer to the chiral effective lagrangian [68–70] as a prototype theory which will also be used for the numerical calculations.

It is preferable here to evaluate V from its relationship with the two-meson irreducible kernel $\widetilde{K}$, (8), which must be considered in its matrix form in the two-channel space. The kernel $\widetilde{K}$ is made of vertices and eventually of loops and may have momentum dependences. By analyzing, with the threshold expansion method [66], its behavior when integrated in (8) with g_0 near the two-particle threshold (three-dimensional integration), one finds that the eventual three-momentum dependences of $\widetilde{K}$ produce after integration momenta in the form $\mathbf{p}^2$ or $\mathbf{q}^2$ multiplying momentum independent pieces. Such terms have additional α^2 contributions with respect to the momentum independent pieces when considered in the QED bound states and thus can be neglected. Concerning the four-dimensional integration with $\widetilde{G}_0$, one notices that the presence of loop momenta in the numerator improves in general the infrared behavior of the integral; in this case it is only the hard momenta, which feel the ultraviolet behavior of the integral, that are concerned by their presence. Therefore, without loss of generality, the infrared behavior of integrals involving the kernel $\widetilde{K}$ can be studied by considering the latter as a constant and its value fixed at the two-meson threshold. In princple, the total energy is fixed at the bound state energy, but since $\widetilde{K}$ is a smooth function of the energy and since the binding energy is of order α^2, one can continue without harm the energy of $\widetilde{K}$ up to threshold. By convention, one chooses for the strong interaction masses in the isospin symmetry limit the charged meson masses.

With the above simplification, the integrations in (8) involve only $\widetilde{G}_0$ and g_0. Here, however, the effective propagators $g_{0\rm c}$ and $g_{0\rm n}$ are defined with the meson physical masses [see (1)]. It is then necessary to carry out a consistent calculation, to also consider the propagators in $\widetilde{G}_0$ with the corresponding physical masses. The details of the integrations are presented in the appendices; see (A.5)–(A.7). A typical one-loop diagram, involving $\widetilde{G}_0$, and its constraint diagram, involving g_0, is presented in Fig. 1.

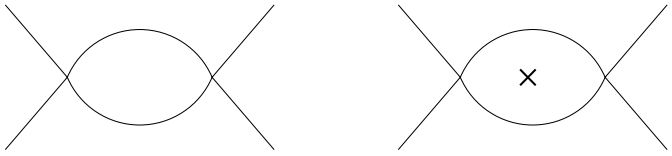

Fig. 1. Two-meson one-loop diagram and its constraint diagram, denoted with a cross

The integration of g_{0c}, at the bound state energy, provides the factor $\sqrt{-b_{0c}^2(s)}/(4\pi)$ [see (A.5)]; it cancels a similar factor present in the integral of $\widetilde{G}_{0c}$ [see (A.6)–(A.7)]. Similarly, the inegration of g_{0n}, at the bound state energy, provides the factor $-\mathrm{i}\sqrt{b_{0n}^2(s)}/(4\pi)$; it cancels the imaginary part of the integral of $\widetilde{G}_{0n}$. The remaining parts of the integrals of $\widetilde{G}_{0c}$ and $\widetilde{G}_{0n}$ are real smooth functions of the energy and can be replaced, dropping $O(\alpha^2)$ corrections, by their values at the charged meson threshold. The above calculations can be repeated with all loops present in (8). One thus recovers the real part of the scattering amplitude at the charged meson threshold. Once the contributions of the effective propagators g_0 have been taken into account, and in order to avoid double-countings, one must take again in the remaining parts of the strong interaction amplitudes the equality of the masses of isospin partners, fixed at the charged meson masses. The effect of mass differences is taken into account separately within the calculations of electromagnetic and isospin symmetry breaking contributions.

In summary, the strong interaction potentials that contribute at first-order perturbation theory to the complex shift of the bound state energy are given by the (charged meson) threshold values of the real parts of the strong interaction scattering amplitudes:

$$\begin{aligned}
&\overline{V}_{\mathrm{cc},h} = V_{\mathrm{cc},h} = \mathcal{R}e\,\widetilde{T}_{\mathrm{cc},h}\Big|_{\mathrm{thr.}}\,,\\
&V_{\mathrm{cn},h} = V_{\mathrm{nc},h} = \mathcal{R}e\,\widetilde{T}_{\mathrm{cn},h}\Big|_{\mathrm{thr.}} = \mathcal{R}e\,\widetilde{T}_{\mathrm{nc},h}\Big|_{\mathrm{thr.}}\,,
\end{aligned} \tag{50}$$

where the subscript h refers to the purely hadronic part of the corresponding quantity. The threshold values of the real parts of the scattering amplitudes are given by the S-wave scattering lengths (33)–(36). One finds

$$\begin{aligned}
&V_{\mathrm{cc},h} = -\frac{4\pi}{3}(2a_0^{1/2} + a_0^{3/2}),\\
&V_{\mathrm{cn},h} = V_{\mathrm{nc},h} = \frac{4\pi}{3}\sqrt{2}\,(a_0^{1/2} - a_0^{3/2})\,.
\end{aligned} \tag{51}$$

Since those potentials are constant in momentum space, they yield delta-functions in x-space and their diagonal matrix elements become proportional to the square of the modulus of the wave function at the origin. In that case, only S-wave states contribute. One finds for the complex energy shift at first order:

$$\begin{aligned}
\mathcal{E}_{h,n\ell}^{(1)} &= E_{h,n\ell}^{(1)} - \frac{\mathrm{i}}{2}\Gamma_{h,n\ell}^{(1)}\\
&= \frac{1}{2\mu}\varphi_{n\ell}^{\dagger}\Big[\, V_{\mathrm{cc},h} + V_{\mathrm{cn},h}\, g_{0\mathrm{n}}\, V_{\mathrm{nc},h}\,\Big]\varphi_{n\ell}\\
&= -\frac{1}{2\mu}\frac{4\pi}{3}\Big[\,\left(2a_0^{1/2} + a_0^{3/2}\right)\\
&\quad + \mathrm{i}\frac{2p_{n0}^*}{3}\left(a_0^{1/2} - a_0^{3/2}\right)^2\,\Big]\Big|\varphi_{n0}(0)\Big|^2\,\delta_{\ell 0}\,,
\end{aligned} \tag{52}$$

where p_{n0}^* is the c.m. momentum of the neutral mesons after the decay of the bound state with quantum numbers $(n, \ell = 0)$. Taking into account that

$$\Big|\varphi_{n\ell}(0)\Big|^2 = \frac{\mu^3\alpha^3}{\pi n^3}\delta_{\ell 0} \tag{53}$$

and introducing the isospin even and odd scattering lengths (34),

$$a_0^+ = \frac{1}{3}\left(a_0^{1/2} + 2a_0^{3/2}\right)\,,\quad a_0^- = \frac{1}{3}\left(a_0^{1/2} - a_0^{3/2}\right)\,, \tag{54}$$

we obtain

$$E_{h,n0}^{(1)} = -2\mu^2\,\frac{\alpha^3}{n^3}\left(a_0^+ + a_0^-\right), \tag{55}$$

$$\Gamma_{h,n0}^{(1)} = 8\,p_{n0}^*\,\mu^2\,\frac{\alpha^3}{n^3}\left(a_0^-\right)^2. \tag{56}$$

The above formulas correspond to the expressions found by Deser et al. [1–4] and provide the leading effects in the shift in the real part of the energy of the bound state and in the width of the decay into the neutral mesons.

Numerical predictions about the scattering lengths are made from chiral perturbation theory (ChPT). They are summarized in Table 1.

On experimental grounds, the values of the scattering lengths are obtained from an extrapolation of high energy data down to the threshold. A complete analysis of the problem, using the Roy [74] and Steiner [75] equations, has given [76]

$$\begin{aligned}
&m_\pi a_0^{1/2} = 0.224 \pm 0.022\,,\\
&m_\pi a_0^{3/2} = -(0.448 \pm 0.077)\times 10^{-1}\,.
\end{aligned} \tag{57}$$

Although the two-loop results of ChPT are not yet well understood [77–79], one notices, with the improvement of the accuracy of the calculations, a reasonable convergence of the theoretical estimates towards the experimental values. We shall adopt the central values of the experimental results (57) for the estimates that we shall do in the subsequent sections for the various corrections to the lowest-order results; uncertainties in these corrections related to the central values will be neglected. For

Table 1. Theoretical predictions for the S-wave scattering lengths from ChPT

ChPT	$m_\pi a_0^{1/2}$	$m_\pi a_0^{3/2}$
Tree [71]	0.14	-0.07
One-loop [72]	0.19 ± 0.02	-0.05 ± 0.02
Two-loop [73]	0.220	-0.047

Table 2. Zeroth-order energies, first-order energy shifts, decay widths and lifetimes of hadronic origin of the first three bound states

$n\,\ell$	$E^{(0)}$ (eV)	$E_h^{(1)}$ (eV)	$\Gamma_h^{(1)}$ (eV)	$\tau_h^{(1)}$ (10^{-15} s)
1 0	−2898.61	−8.86	0.175	3.76
2 0	−724.65	−1.11	0.022	30.09
2 1	−724.65	0.00	0.000	∞

the present lowest-order results we obtain for the first three bound states the following estimates for the energies, decay widths and lifetimes (τ), presented in Table 2.

In the following, we shall evaluate $O(\alpha)$ corrections to these results. They originate from three effects: the pure electromagnetic interaction, electromagnetic radiative corrections to the strong interaction and second-order perturbation theory effects of the bound state energy expansion. We shall consider them separately.

5 Electromagnetic interaction

In this section we consider mainly corrections coming from the pure electromagnetic interaction. They arise in the channel $\pi^-K^+ \to \pi^-K^+$ from one- and two-photon exchange diagrams and also include vacuum polarization contribution. The corresponding diagrams, together with the constraint diagram of the box-ladder diagram, are represented in Fig. 2. Vertex correction diagrams, associated with self-energy diagrams, contribute only at order $\alpha^5 \ln \alpha^{-1}$ and may be ignored at the present level of precision (order α^4).

The on-mass shell one-photon exchange diagram (a) gives the contribution

$$V_{\mathrm{cc},1\gamma} = \frac{1}{2\sqrt{s}} \frac{e^2}{t} \Big(2 \left(s - m_{\pi^-}^2 - m_{K^+}^2 \right) + t \Big) \qquad (58)$$

[$e^2 = 4\pi\alpha$], from which one has to subtract the Coulomb potential (39). An expansion of the total energy, according to (37), should also be made.

In the category of two-photon exchange diagrams, we isolate the box-ladder, crossed-ladder and constraint diagrams, (b)–(d). The box-ladder and crossed-ladder diagrams have separately infrared divergences, as well as spurious singularities at threshold. To avoid their appearance, one must consider the sum of the above three diagrams, within which several mutual cancellations occur. The mechanism of cancellation is best understood with the threshold expansion method [66]. The leading part of potential momenta contribution, of order $\alpha^2 \ln \alpha^{-1}$, coming from the box-ladder diagram, is cancelled by that of the constraint diagram. The next-to-leading term, of order α^4, vanishes in four dimensions. Ultrasoft momenta do not contribute on the mass shell. Soft momenta contributions of box-ladder and crossed-ladder diagrams, of order $\alpha^3 \ln \alpha^{-1}$, cancel each other. One remains with $O(\alpha^4)$ terms, the sum of which also vanishes on the mass shell. Therefore, the sum of the three diagrams (b)–(d) does not contribute at order α^4. Details can be found in the appendix.

The two-photon exchange diagrams have generally ultraviolet divergences. The counterterm lagrangian, which is a four-meson contact interaction term, does not contribute at order α^4.

Diagrams (e) and (f) contribute at order α^4. The sum of their contribution is (A.18):

$$V_{\mathrm{cc},2\gamma} = -\frac{(m_{\pi^-} + m_{K^+})}{8\sqrt{s}} \frac{e^4}{\sqrt{-t}}\,. \qquad (59)$$

Diagram (g) does not contribute at order α^4.

The total corrective contribution of one- and two-photon exchange diagrams (without vacuum polarization), $V_{\mathrm{cc},1\gamma}$ minus the Coulomb potential (39) and $V_{\mathrm{cc},2\gamma}$, taking also into account the kinematic energy correction factor coming from the relativistic wave equation operator (last term of (49)), is:

$$E^{(1)}_{(1+2)\gamma,n\ell} = \frac{\mu}{8} \Big(3 - \frac{\mu}{(m_{\pi^-} + m_{K^+})} \Big) \frac{\alpha^4}{n^4} + \frac{\mu^2}{(m_{\pi^-} + m_{K^+})} \frac{\alpha^4}{n^3} \delta_{\ell 0} - \frac{\mu \alpha^4}{n^3 (2\ell + 1)}. \qquad (60)$$

This coincides with similar results obtained from the Bethe–Salpeter equation (in the Coulomb gauge) [80] and from the Breit equation [46].

Another electromagnetic contribution is represented by the vacuum polarization diagram (h). Generally, in

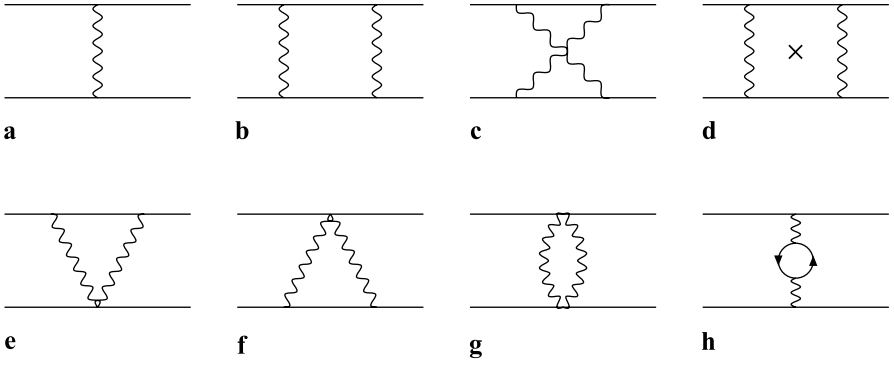

Fig. 2. One- and two-photon exchange diagrams contributing to the pure electromagnetic corrections. The diagram with a cross represents the constraint diagram

positronium, this diagram contributes at order $O(\alpha^5)$. However, due to the mass differences between the electron, entering in the internal loop, and mesons, the contribution of the vacuum polarization diagram becomes enhanced [24]. It is numerically situated for the energy shift between $O(\alpha^3)$ and $O(\alpha^4)$ and turns out to be the most important correction to the strong interaction effect. It can be evaluated analytically [16, 31, 32]. We have evaluated it numerically for the first three bound states, from the expression of the corresponding local potential [81]. The results are compatible with the analytic evaluations and are presented below in Table 3.

Apart from the pure electromagnetic corrections, we shall also evaluate here the strong interaction contributions to the meson electromagnetic form factors. The reason is that the interference effects between strong interaction and electromagnetism in the scattering amplitudes are evaluated in the literature without the above form factors, which are considered as parts of the one-photon exchange diagram (see Fig. 3).

Defining the hadronic part of the electromagnetic form factor of pseudoscalar mesons as [69]

$$F_V(t) = 1 + \frac{1}{6}\langle r^2\rangle t + O\left(t^2\right), \tag{61}$$

where $\langle r^2\rangle$ defines the mean square charge radius of the meson, the corresponding contribution through the one-photon exchange diagram is:

$$V_{\mathrm{cc,hff}} = 2\mu e^2 \frac{1}{6}\langle r^2\rangle . \tag{62}$$

Table 3. Electromagnetic corrections (elm) to the energy shift, composed of contributions of one- and two-photon exchanges ($(1+2)\gamma$), vacuum polarization (vpol) and hadronic form factors (hff)

$n\ \ell$	$E^{(1)}_{(1+2)\gamma}$ (eV)	$E^{(1)}_{\mathrm{vpol}}$ (eV)	$E^{(1)}_{\mathrm{hff}}$ (eV)	$E^{(1)}_{\mathrm{elm}}$ (eV)
1 0	−0.147	−2.561	0.051	−2.657
2 0	−0.025	−0.296	0.006	−0.315
2 1	−0.006	−0.025	0.000	−0.031

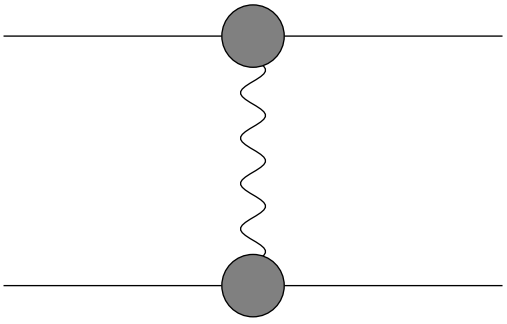

Fig. 3. Strong interaction contribution to the electromagnetic form factors of mesons

[hff: hadronic form factor.] The sum of the contributions of the π and K mesons to the energy shift is

$$E^{(1)}_{\mathrm{hff},n\ell} = \frac{2}{3}\mu^3 \frac{\alpha^4}{n^3}\left(\langle r^2\rangle_{\pi^-} + \langle r^2\rangle_{K^+}\right)\delta_{\ell 0} . \tag{63}$$

The mean square radii of the π and K mesons were calculated from the data in [82] in the framework of ChPT to two loops. The values found there, which we use for the numerical evaluations, are the following:

$$\begin{aligned}\langle r^2\rangle_{\pi^-} &= (0.452 \pm 0.013)\ \mathrm{fm}^2,\\ \langle r^2\rangle_{K^+} &= (0.363 \pm 0.072)\ \mathrm{fm}^2 .\end{aligned} \tag{64}$$

Numerical estimates of the various electromagnetic contributions to the first three bound states are summarized in Table 3.

6 Strong interaction in the presence of electromagnetism

To complete the evaluation of corrections at first order of perturbation theory, we have now to consider the interference effects between strong interaction and electromagnetism, including isospin symmetry breaking. Since we are interested in $O(\alpha)$ corrections to the strong interaction effects found in Sect. 4, it is sufficient to consider diagrams with a one-photon propagator. The analysis is best carried out starting from the general relationship of the potential V with the two-meson irreducible kernel $\widetilde{K}$ [see (8)], which was already used in the pure strong interaction case.

The kernel $\widetilde{K}$ can be separated into three parts, pure hadronic, $\widetilde{K}_h$, pure electromagnetic, $\widetilde{K}_\gamma$, and a part with interference between both, $\widetilde{K}_{h\gamma}$: $\widetilde{K} = \widetilde{K}_h + \widetilde{K}_\gamma + \widetilde{K}_{h\gamma}$. Replacing $\widetilde{K}$ in (8) and then linearizing with respect to $\widetilde{K}_\gamma + \widetilde{K}_{h\gamma}$ and subtracting the pure hadronic potential and the pure electromagnetic kernel $\widetilde{K}_\gamma$, one ends up with the expression of the interference potential:

$$\begin{aligned}V_{h\gamma} = &\left(1 - \widetilde{K}_h\left(\widetilde{G}_0 - g_0\right)\right)^{-1}\left(\widetilde{K}_\gamma + \widetilde{K}_{h\gamma}\right)\\ &\times\left(1 - \left(\widetilde{G}_0 - g_0\right)\widetilde{K}_h\right)^{-1} - \widetilde{K}_\gamma .\end{aligned} \tag{65}$$

Retaining the first few terms, we have for $V_{h\gamma}$ an expansion as follows:

$$\begin{aligned}V_{h\gamma} = &\widetilde{K}_{h\gamma} + \widetilde{K}_h\left(\widetilde{G}_0 - g_0\right)\widetilde{K}_\gamma + \widetilde{K}_\gamma\left(\widetilde{G}_0 - g_0\right)\widetilde{K}_h\\ &+ \widetilde{K}_h\left(\widetilde{G}_0 - g_0\right)\widetilde{K}_\gamma\left(\widetilde{G}_0 - g_0\right)\widetilde{K}_h + \cdots\end{aligned} \tag{66}$$

In the present approximation, $\widetilde{K}_\gamma$ is the one-photon exchange kernel; also $\widetilde{K}_{h\gamma}$ contains effects of isospin symmetry breaking; internal propagators, such as $\widetilde{G}_0$, should be considered with physical masses.

Typical diagrams, in the charged–charged (cc) channel, are represented in Fig. 4.

Diagrams (a)–(c) represent one-photon exchanges in the t-channel, u-channel and s-channel respectively; diagram (d) is the constraint diagram of diagram (c). Also

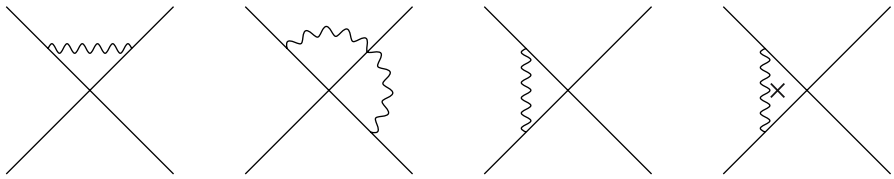

Fig. 4. Electromagnetic radiative corrections to the strong interaction in the charged–charged channel; diagram **d** is the constraint diagram of diagram **c**; diagrams symmetric to those, as well as self-energy diagrams, are not drawn

four other diagrams symmetric to the above ones exist; futhermore, one must also include the contributions of the self-energy diagrams. Each of those diagrams has infrared divergences on the mass shell; however, mutual cancellations occur by grouping several diagrams. The sum of the t-channel diagrams and the contributions of the self-energy diagrams is finite at order α^4. The constraint diagram cancels the infrared divergence and spurious singularities of the s-channel diagram generated by the potential momenta [66]. The remaining part of the s-channel diagram, which is still infrared divergent and generated by the hard momenta, is associated with the u-channel diagram, which has similar singularities; their sum is free of divergences and of spurious singularities. Diagrams where the photon is emitted from the vertex (not drawn in Fig. 4) are not infrared singular and contribute as $O(\alpha^4)$. The sum of all the above diagrams is infrared finite and of order α^4. It defines the regularized real part of the strong interaction vertex in the presence of electromagnetism; its value at the bound state energy differs from its value at threshold by an $O(\alpha^2)$ term and therefore can be replaced by the value of the regularized real part of the vertex at threshold. (See the appendix for details.)

In the charged–neutral (cn) or neutral–charged (nc) channels, t-channel and u-channel type diagrams are absent. In that case, one has to associate the part of the s-channel diagram generated by the hard momenta with the self-energy contributions of the external charged particles and the same type of cancellations as above operate, leading to the same qualitative result.

The analysis done above can be repeated with more complicated diagrams. One has always to group several diagrams of the same class to reach, with the aid of the threshold expansion method [66], mutual cancellations of infrared divergences and spurious singularities. The final results that we obtain are very similar to those found in Sect. 4, (50), with the only difference that the pure strong interaction scattering amplitude is now replaced by the regularized strong interaction amplitude in the presence of electromagnetism and isospin symmetry breaking:

$$\begin{aligned}\overline{V}_{\mathrm{cc},h+h\gamma} &= V_{\mathrm{cc},h+h\gamma} = \mathcal{R}e\,\widetilde{T}^{\mathrm{reg.}}_{\mathrm{cc},h+h\gamma}\Big|_{\mathrm{thr.}}\,,\\ V_{\mathrm{cn},h+h\gamma} &= V_{\mathrm{nc},h+h\gamma} = V_{\mathrm{cn}} = V_{\mathrm{nc}}\\ &= \mathcal{R}e\,\widetilde{T}^{\mathrm{reg.}}_{\mathrm{cn}}\Big|_{\mathrm{thr.}} = \mathcal{R}e\,\widetilde{T}^{\mathrm{reg.}}_{\mathrm{nc}}\Big|_{\mathrm{thr.}}\,. \end{aligned} \tag{67}$$

The threshold values of the regularized real parts of the strong interaction scattering amplitudes in the presence of electromagnetism deviate from the strong interaction S-wave scattering lengths (51) by small amounts that we designate by $(\Delta(a_0^+ + a_0^-))_{h\gamma}$ and $(\Delta a_0^-)_{h\gamma}$. One then has

$$\begin{aligned} V_{\mathrm{cc},h+h\gamma} &= -4\pi\left(\left(a_0^+ + a_0^-\right) + \left(\Delta\left(a_0^+ + a_0^-\right)\right)_{h\gamma}\right),\\ V_{\mathrm{cn}} &= 4\pi\sqrt{2}\left(a_0^- + \left(\Delta a_0^-\right)_{h\gamma}\right), \end{aligned} \tag{68}$$

where a_0^+ and a_0^- are the pure strong interaction isospin even and odd scattering lengths, respectively (54). For further use, we define the following relative amounts:

$$\delta^{(1)}_{\mathrm{cc},h\gamma} \equiv \frac{\left(\Delta\left(a_0^+ + a_0^-\right)\right)_{h\gamma}}{\left(a_0^+ + a_0^-\right)}, \qquad \delta^{(1)}_{\mathrm{cn},h\gamma} \equiv \frac{\left(\Delta a_0^-\right)_{h\gamma}}{a_0^-}\,. \tag{69}$$

The various diagrams entering in the calculation of the strong interaction scattering amplitude in the presence of electromagnetism have also ultraviolet divergences. They are eliminated by the low energy constants of the effective chiral lagrangian in the presence of electromagnetism [83, 84].

Turning back to the infrared problem, we emphasize the following point. The constraint diagrams have eliminated, to order α^4, the infrared divergences and threshold singularities of the scattering amplitudes and allowed the definition of regularized real parts of them. In the literature, the scattering amplitudes are generally calculated in the scattering region; then, infrared divergences are eliminated by factorizing the Coulomb phase [85], which does not contribute to the cross section, and by combining the process under consideration with real soft photon emission processes [84, 86–89]. The remaining threshold singularities are then subtracted to define a regularized scattering amplitude at threshold. In the present formalism, the use of constraint diagrams for the definition of the potentials circumvents the latter procedures on the mass shell (to order α^4), providing directly the regularized result. It can be checked explicitly that the pieces that are cancelled by the constraint diagrams are the same quantities that are subtracted in procedures dealing with the scattering amplitudes in the scattering region. Therefore, the regularized real parts of the amplitudes that we have defined in (67) are identical to those defined in the literature.

More complicated diagrams than those of Fig. 4 involve an increasing number of loops. However, in ChPT, the increase in the number of loops decreases the order of magnitude of the corresponding correction at low energy; this is why the chiral perturbation theory is organized in terms of the number of loops [68–70]. Therefore, the diagrams of the type of Fig. 4 represent the most important contributions to the interference effects between strong interaction and

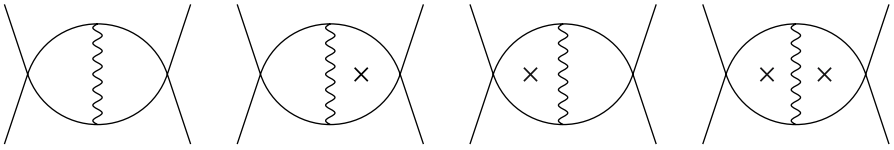

Fig. 5. Two-loop diagram and its constraint diagrams

electromagnetism, apart from isospin partner mass difference insertion terms at the tree level, and practical calculation of these effects have been limited to them [84, 86–89]. Next-to-leading effects are represented by diagrams of the type of Fig. 5. The latter diagrams contain infrared logarithmic contributions which partially enhance their order of magnitude and will be taken into account in Sect. 8 in conjunction with second-order perturbation theory effects.

The evaluation for the πK atom of contributions of diagrams of the type of Fig. 4 and of mass shift insertion effects have been done by two groups of authors [86–89]. Although their results do not exactly coincide, the numerical values that emerge for the corrective terms are close to each other. We use here the numerical values given in [88, 89]. One has

$$\begin{aligned}\delta^{(1)}_{\mathrm{cc},h\gamma} &= O\left(e^2\right) + O\left(e^2\,p^2\right) + O\big(\,|m_u - m_d|\,p^2\,\big)\\ &= (1.2 - (0.3 \pm 3.2) + 0.2) \times 10^{-2}\\ &= (1.1 \pm 3.2) \times 10^{-2}, \end{aligned} \tag{70}$$

$$\begin{aligned}\delta^{(1)}_{\mathrm{cn},h\gamma} &= O\left(e^2\right) + O\left(\,|m_u - m_d|\,\right) + O\left(e^2\,p^2\right)\\ &\quad + O\big(\,|m_u - m_d|\,p^2\,\big)\\ &= (0.8 + 0.5 - (0.8 \pm 0.7) + (0.7 \pm 0.2)) \times 10^{-2}\\ &= (1.2 \pm 0.7) \times 10^{-2}, \end{aligned} \tag{71}$$

where $O(e^2)$ and $O\big(\,|m_u - m_d|\,\big)$ represent effects of electromagnetism and isospin symmetry breaking mass insertions at the tree level, $O(e^2\,p^2)$ and $O\big(\,|m_u - m_d|\,p^2\,\big)$ effects of electromagnetism and isospin symmetry breaking at one-loop level; the uncertainties arise mainly from the electromagnetic low energy constants of the effective chiral lagrangian, which are estimated by their order of magnitude. (We have added uncertainties quadratically in (71).)

The above modifications of threshold values of the amplitudes modify the results (55) and (56), obtained in the pure strong interaction case, with the inclusion of the corresponding corrections:

$$\begin{aligned}E^{(1)}_{h+h\gamma,n0} &= -2\mu^2\,\frac{\alpha^3}{n^3}\left(a_0^+ + a_0^-\right)\left(1 + \delta^{(1)}_{\mathrm{cc},h\gamma}\right)\\ &= E^{(1)}_{h,n0}\left(1 + \delta^{(1)}_{\mathrm{cc},h\gamma}\right)\\ &= E^{(1)}_{h,n0}\,\left(1 + (1.1 \pm 3.2) \times 10^{-2}\right), \end{aligned} \tag{72}$$

$$\begin{aligned}\Gamma^{(1)}_{h+h\gamma,n0} &= 8\,p^*_{n0}\,\mu^2\,\frac{\alpha^3}{n^3}\left(a_0^-\right)^2\left(1 + 2\delta^{(1)}_{\mathrm{cn},h\gamma}\right)\\ &= \Gamma^{(1)}_{h,n0}\left(1 + 2\delta^{(1)}_{\mathrm{cn},h\gamma}\right)\\ &= \Gamma^{(1)}_{h,n0}\,\left(1 + (2.4 \pm 1.4) \times 10^{-2}\right). \end{aligned} \tag{73}$$

7 Cancellation of divergences of three-dimensional diagrams

We shall show in this section that divergences of constraint diagrams do not appear in physical quantities. Up to order α^4 effects, the only divergences that are introduced by constraint diagrams are those that cancel the infrared divergences of the on-mass shell scattering amplitudes. Other divergences that might appear in the perturbation series of the energy shifts are actually mutually cancelled.

To observe the latter property, we go back to the matrix notation and express directly the scattering amplitude $\widetilde{T}'_2$ [see (21)], that defines the perturbation expansion of the energy shifts (24), in terms of two-particle irreducible kernels. Let $\widetilde{K}_1$ be the two-particle irreducible kernel of the unperturbed theory, that defines the potential V_1; we have

$$V_1 = \widetilde{K}_1\left(1 - (\widetilde{G}_0 - g_0)\widetilde{K}_1\right)^{-1}. \tag{74}$$

The potential V_2 is defined by $V_2 = V - V_1$, where V is the potential corresponding to the total interaction. It is related to the total scattering amplitude $\widetilde{T}$ [see (3)] and to its two-particle irreducible kernel $\widetilde{K}$ [see (8)], which in turn can be separated into two parts, after isolating in it $\widetilde{K}_1$:

$$\widetilde{K} = \widetilde{K}_1 + \widetilde{K}_2\,. \tag{75}$$

For the Green function $\widetilde{G}'_1$ that enters in the definition of $\widetilde{T}'_2$ [see (21)], one can use a decomposition similar to that of (44):

$$G'_1 = g_0 + g_0 V_1 g_0 + G''_1\,, \tag{76}$$

where G''_1 corresponds to the part created by multiparticle or multiphoton exchanges.

Replacing then V_1 and V in the expression of $\widetilde{T}'_2$ in terms of $\widetilde{K}_1$ and $\widetilde{K}$, respectively, and iterating $\widetilde{T}'_2$ and $\widetilde{G}'_1$, one obtains for $\widetilde{T}'_2$ the following expansion, in which we have kept up to two propagator terms:

$$\begin{aligned}\widetilde{T}'_2 = {} & \widetilde{K}_2 + \widetilde{K}_2\widetilde{G}_0\widetilde{K}_2 + \widetilde{K}_2\widetilde{G}_0\widetilde{K}_2\widetilde{G}_0\widetilde{K}_2 + \widetilde{K}_2\widetilde{G}_0\widetilde{K}_1\widetilde{G}_0\widetilde{K}_2\\ & + \widetilde{K}_2\widetilde{G}''_1\widetilde{K}_2 + \widetilde{K}_1\left(\widetilde{G}_0 - g_0\right)\widetilde{K}_2 + \widetilde{K}_2\left(\widetilde{G}_0 - g_0\right)\widetilde{K}_1\\ & + \widetilde{K}_1\left(\widetilde{G}_0 - g_0\right)\widetilde{K}_2\widetilde{G}_0\widetilde{K}_2 + \widetilde{K}_2\widetilde{G}_0\widetilde{K}_2\left(\widetilde{G}_0 - g_0\right)\widetilde{K}_1\\ & + \widetilde{K}_1\left(\widetilde{G}_0 - g_0\right)\widetilde{K}_1\left(\widetilde{G}_0 - g_0\right)\widetilde{K}_2\\ & + \widetilde{K}_2\left(\widetilde{G}_0 - g_0\right)\widetilde{K}_1\left(\widetilde{G}_0 - g_0\right)\widetilde{K}_1\\ & + \widetilde{K}_1\left(\widetilde{G}_0 - g_0\right)\widetilde{K}_2\left(\widetilde{G}_0 - g_0\right)\widetilde{K}_1 + \cdots \end{aligned} \tag{77}$$

The important point to be noticed is that the effective propagator g_0 is completely absent in terms containing only the kernel $\widetilde{K}_2$. g_0 is present in terms that contain $\widetilde{K}_1$ on their left or right boundaries. Since the higher-order electromagnetic corrections with respect to the Coulomb potential appear at order α^4 only at first order of perturbation theory, one may simplify the analysis by assuming that $\widetilde{K}_1$ corresponds essentially to the pure elecromagnetic part, $\widetilde{K}_\gamma$, and $\widetilde{K}_2$ to the pure hadronic part, $\widetilde{K}_h$, as well as to the interference part of the hadronic and electromagnetic interactions, $\widetilde{K}_{h\gamma}$. The terms $\widetilde{K}_1\widetilde{G}_0\widetilde{K}_2$ or $\widetilde{K}_2\widetilde{G}_0\widetilde{K}_1$, in which $\widetilde{K}_2$ is represented by a constant contact term, have infrared divergences, the dominant part of which is cancelled by the constraint propagator g_0; the non-dominant divergences are mutually cancelled, by considering together self-energy diagrams and eventually other combinations of t-channel and u-channel diagrams (cf. Sect. 6). The term $\widetilde{K}_2\widetilde{G}_0\widetilde{K}_1\widetilde{G}_0\widetilde{K}_2$, which in lowest order is represented by diagram (a) of Fig. 5, is finite and actually its constraint diagrams (b)–(d) of Fig. 5 have been cancelled by similar terms that have appeared through the perturbative expansion of the bound state energy. Similarly, the constraint diagrams which were present in the definition of the hadronic potentials V_h (Sect. 3) also disappeared. Those diagrams, considered individually, contain ultraviolet or infrared divergences (linear or logarithmic). The present cancellation mechanism shows that their effect is irrelevant. However, the way of organizing the perturbation expansion in terms of the potentials V, rather than in terms of the kernels $\widetilde{K}$ or the amplitudes $\widetilde{T}$, has the advantage, through cancellation effects by constraint diagrams, of naturally arriving at quantities that are smooth functions of the energy in the vicinity of the two-particle threshold, being continued, within the present approximations, to threshold (cf. (50) and (67)). Actually, it is only the finite parts of their contributions that are relevant for that operation. This is why we shall continue formulating the perturbative expansion of the bound state energy in terms of potentials, keeping in mind that in mutually cancelling constraint diagrams the same convention should be used when removing divergences.

In summary, no ultraviolet or infrared divergences globally occur from three-dimensional diagrams in physical quantities up to oreder α^4.

8 Second order of perturbation theory

We evaluate, in this section, the contributions of second-order perturbation theory effects, which are represented by the terms containing the subtracted Coulomb Green function $G'_{\rm C}$ in (49). Here, the potentials that have significant contributions are the hadronic part and the vacuum polarization part of $\overline{V}_{\rm cc}$.

We first consider the hadronic part $V_{{\rm cc},h}$ of $\overline{V}_{\rm cc}$, which was already studied in Sect. 4. Its contribution to the energy shift at second-order of perturbation theory is represented by the following sum of terms:

$$2\mu\mathcal{E}^{(2)}_{hh,n\ell} = \varphi^\dagger_{n\ell}\Big[V_{{\rm cc},h}\frac{G'_{\rm C}}{2\mu}V_{{\rm cc},h} + V_{{\rm cc},h}\frac{G'_{\rm C}}{2\mu}V_{{\rm cn},h}g_{0{\rm n}}V_{{\rm nc},h} + V_{{\rm cn},h}g_{0{\rm n}}V_{{\rm nc},h}\frac{G'_{\rm C}}{2\mu}V_{{\rm cc},h}\Big]\varphi_{n\ell}\,. \tag{78}$$

(A negligible contribution, involving two $g_{0{\rm n}}$s, has been omitted.) Since at the approximation we are working $V_{{\rm cc},h}$ and $V_{{\rm cn},h}$ are constants in momentum space (51), the contribution of $G'_{\rm C}$ factorizes with its integrations, and the wave functions become projected on their values at the origin in x-space:

$$2\mu\mathcal{E}^{(2)}_{hh,n\ell} = V_{{\rm cc},h}\left[\int\frac{{\rm d}^3p}{(2\pi)^3}\frac{{\rm d}^3p'}{(2\pi)^3}\frac{1}{2\mu}G'_{\rm C}\left(E^{(0)}_{n\ell},\mathbf{p},\mathbf{p}'\right)\right] \times|\varphi_{n\ell}(0)|^2\,\left[\,V_{{\rm cc},h}+2V_{{\rm cn},h}\,g_{0{\rm n}}\,V_{{\rm nc},h}\,\right]\,. \tag{79}$$

Defining

$$\left\langle\frac{G'_{\rm C}}{2\mu}\right\rangle_{n\ell} \equiv \int\frac{{\rm d}^3p}{(2\pi)^3}\frac{{\rm d}^3p'}{(2\pi)^3}\frac{1}{2\mu}G'_{\rm C}\left(E^{(0)}_{n\ell},\mathbf{p},\mathbf{p}'\right)\,, \tag{80}$$

$$\delta^{(2)}_{hh,n\ell} \equiv V_{{\rm cc},h}\left\langle\frac{G'_{\rm C}}{2\mu}\right\rangle_{n\ell}\,, \tag{81}$$

and taking into account the results (51), (52), (55) and (56) one obtains

$$\mathcal{E}^{(2)}_{hh,n\ell} = E^{(2)}_{hh,n\ell} - \frac{\rm i}{2}\Gamma^{(2)}_{hh,n\ell} = \delta^{(2)}_{hh,n0}\left(E^{(1)}_{h,n0} - {\rm i}\Gamma^{(1)}_{h,n0}\right)\delta_{\ell 0}\,, \tag{82}$$

which in turn yields

$$\frac{E^{(2)}_{hh,n0}}{E^{(1)}_{h,n0}} = \delta^{(2)}_{hh,n0}\,,\qquad \frac{\Gamma^{(2)}_{hh,n0}}{\Gamma^{(1)}_{h,n0}} = 2\delta^{(2)}_{hh,n0}\,. \tag{83}$$

The calculation therefore amounts to that of the double integral of $G'_{\rm C}/(2\mu)$. The latter is composed of the three contributions in (44).

The first corresponds to zero-photon exchange and its integral is equal to that of $g_{0{\rm c}}$, i.e., to $\sqrt{-b^2_{0{\rm c}}(s)}/(4\pi)$ [see (A.5)].

The second term corresponds to one-photon exchange; its integral is ultraviolet divergent, but this divergence is cancelled by that of the three constraint diagrams of Fig. 5 (see the appendix for details). The finite part of the latter in turn cancels a finite logarithmic piece of the four-dimensional diagram (a) of Fig. 5; therefore, the finite part of the sum of the four diagrams of Fig. 5 becomes a smooth function. The finite part of the one-photon exchange part of the integral of $G'_{\rm C}/(2\mu)$ simply isolates the dominant logarithmic part of the four-dimensional diagram.

The third term corresponds to the multiphoton exchanges and is finite. It can be calculated in several ways: either using an integration by parts in the variable ρ and isolating first the pole term to be subtracted [90], or integrating first with respect to the momenta and isolating at the end the pole term.

The result is, for the finite part, using dimensional regularization and writing the contributions of the above three terms in successive order:

$$\left\langle \frac{G'_{\rm C}}{2\mu} \right\rangle_{n0} = \frac{\mu\alpha}{4\pi}\frac{1}{n} - \frac{\mu\alpha}{2\pi}\ln\left(\frac{n}{\alpha}\right) + \frac{\mu\alpha}{2\pi}\left(\psi(n) - \psi(1) - \frac{3}{2n}\right), \tag{84}$$

where ψ is the logarithmic derivative of the Gamma function.

Numerically, one finds, using (51),

$$\delta^{(2)}_{hh,10} = 0.009, \quad \delta^{(2)}_{hh,20} = 0.008\,. \tag{85}$$

We next consider the interference term between the hadronic and vacuum polarization parts of $\overline{V}_{\rm cc}$. The corresponding energy shift is:

$$2\mu\mathcal{E}^{(2)}_{{\rm hvpol},n\ell} = 2\varphi^\dagger_{n\ell} V_{{\rm cc,vpol}} \frac{G'_{\rm C}}{2\mu}\Big[V_{{\rm cc},h} + V_{{\rm cn},h} g_{0{\rm n}} V_{{\rm nc},h}\Big]\varphi_{n\ell}, \tag{86}$$

which gives, using (52):

$$\begin{aligned}\mathcal{E}^{(2)}_{{\rm hvpol},n\ell} &= E^{(2)}_{{\rm hvpol},n\ell} - \frac{\rm i}{2}\Gamma^{(2)}_{{\rm hvpol},n\ell} \\ &= 2\Big(\varphi^\dagger_{n0}\, V_{\rm cc,vpol}\, \frac{G'_{\rm C}}{2\mu}\Big)\, \frac{1}{\varphi^\dagger_{n0}(0)} \\ &\quad \times \Big(\, E^{(1)}_{h,n0} - \frac{\rm i}{2}\Gamma^{(1)}_{h,n0}\Big)\,\delta_{\ell 0}\,. \end{aligned} \tag{87}$$

Defining

$$\delta^{(2)}_{{\rm hvpol},n0} \equiv \Big(\varphi^\dagger_{n0}\, V_{\rm cc,vpol}\, \frac{G'_{\rm C}}{2\mu}\Big)\, \frac{1}{\varphi^\dagger_{n0}(0)}, \tag{88}$$

one has

$$\frac{E^{(2)}_{{\rm hvpol},n0}}{E^{(1)}_{h,n0}} = 2\delta^{(2)}_{{\rm hvpol},n0}, \quad \frac{\Gamma^{(2)}_{{\rm hvpol},n0}}{\Gamma^{(1)}_{h,n0}} = 2\delta^{(2)}_{{\rm hvpol},n0}\,. \tag{89}$$

The above correction is finite. Using the expression of the vacuum polarization potential $V_{\rm cc,vpol}$ [81] and replacing $G'_{\rm C}$ by a sum of contributions of intermediate states (discrete and continuous), one finds

$$\begin{aligned}\delta^{(2)}_{{\rm hvpol},10} &= 0.30\alpha \simeq 0.002, \\ \delta^{(2)}_{{\rm hvpol},20} &= 0.28\alpha = 0.002. \end{aligned} \tag{90}$$

On comparing the orders of magnitude of the individual contributions of $V_{{\rm cc},h}$ and $V_{\rm cc,vpol}$ from results (85) and (90), one deduces that the ratio of the contributions of the latter to the former is of the order of 1/4; this implies that the contribution of the quadratic piece in $V_{\rm cc,vpol}$ is in the ratio of 1/16 with respect to the quadratic piece of $V_{{\rm cc},h}$, and hence can be neglected.

9 Summary of results

We calculated the main corrections to the lowest-order formulas of the energy shift and decay width of the πK atom. At lowest order, the energy shift and the decay width are given by the formulas obtained by Deser et al. (Sect. 4). They are expressed in terms of the S-wave scattering lengths of the strong interaction $\pi K \to \pi K$ scattering amplitudes, taken in the isospin symmetry limit; they are designated by $E^{(1)}_{h,n0}$ and $\Gamma^{(1)}_{h,n0}$, where n is the principal quantum number and ℓ (here equal to zero) the orbital quantum number.

The main corrections, of order α, that arise are the following.

1. Pure electromagnetic interaction effects beyond the Coulomb potential, designated by $E^{(1)}_{{\rm elm},n\ell}$ (Sect. 5) in the bound state with quantum numbers n and ℓ. They contribute only to the real energy shift.
2. Electromagnetic radiative corrections as well as isospin symmetry breaking corrections to the strong interaction scattering amplitudes, the relative amounts of which with respect to the lowest-order results are designated by $\delta^{(1)}_{{\rm cc},h\gamma}$ and $\delta^{(1)}_{{\rm cn},h\gamma}$, according to the charged-charged ($\pi^- K^+ \to \pi^- K^+$) and charged–neutral ($\pi^- K^+ \to \pi^0 K^0$) channels (Sect. 6).
3. Corrections coming from second-order perturbation theory of the expansion of the bound state energies (Sect. 8). They involve strong interaction type correlations, represented by the relative amount $\delta^{(2)}_{hh,n0}$ with respect to the lowest-order results, and strong interaction-vacuum polarization type correlations, represented by the relative amount $\delta^{(2)}_{{\rm hvpol},n0}$.

The real energy shift, ΔE, and the decay width, Γ, including the $O(\alpha)$ corrections, take the following expressions:

$$\begin{aligned}\Delta E_{n0} &= -2\mu^2\frac{\alpha^3}{n^3}\left(a_0^+ + a_0^-\right) \\ &\quad \times \Big(\,1 + \delta^{(1)}_{{\rm cc},h\gamma} + \delta^{(2)}_{hh,n0} + 2\delta^{(2)}_{{\rm hvpol},n0}\Big) \\ &\quad + E^{(1)}_{{\rm elm},n0}, \end{aligned} \tag{91}$$

$$\Delta E_{n1} = E^{(1)}_{{\rm elm},n1}, \tag{92}$$

$$\begin{aligned}\Gamma_{n0} &= 8p^*_{n0}\mu^2\frac{\alpha^3}{n^3}\left(a_0^-\right)^2 \\ &\quad \times \Big(\,1 + 2\delta^{(1)}_{{\rm cn},h\gamma} + 2\delta^{(2)}_{hh,n0} + 2\delta^{(2)}_{{\rm hvpol},n0}\Big), \end{aligned} \tag{93}$$

where the S-wave scattering lengths a_0^+ and a_0^- are those of the pure strong interaction theory taken in the isospin symmetry limit, μ the reduced mass of π^- and K^+ and p^*_{n0} the c.m. momentum of the neutral mesons after the decay of the bound state with quantum numbers $(n, \ell = 0)$.

The numerical values of the various corrective terms for the first three bound states are summarized in Table 4.

The uncertainties come mainly from the low energy constants of ChPT in the presence of electrmagnetism which are poorly known and are taken into account through their order of magnitude.

Table 4. Numerical values of the corrective terms to the lowest-order formulas for the first three bound states

$n\ \ell$	$\delta^{(1)}_{cc,h\gamma}$	$\delta^{(1)}_{cn,h\gamma}$	$\delta^{(2)}_{hh}$	$\delta^{(2)}_{\rm hvpol}$	$E^{(1)}_{\rm elm}$(eV)
1 0	0.011 ± 0.032	0.012 ± 0.007	0.009	0.002	-2.66
2 0	0.011 ± 0.032	0.012 ± 0.007	0.008	0.002	-0.32
2 1	0.00	0.00	0.000	0.000	-0.03

The corrective terms have been evaluated using in them the central values of the scattering lengths given by (57). It is evident that they are weakly sensitive to the precise values of the scattering lengths; changes of the order of 10% in the values of the latter quantities would induce only changes of the order of 10^{-3} in the corrective terms. One therefore can safely replace in (91) and (93) the corrective terms by their numerical values and isolate the leading factors of the strong interaction scattering lengths.

The analytic results found in the present paper are the same as those of [35, 36] at the order of approximations that are utilized. The apparent differences that exist in some formulas or in some numerical quantities concern either terms that are of higher order, and hence are numerically negligible, or terms that have been evaluated numerically in a different way, due to the existing large uncertainties in the values of the electromagnetic low energy constants. The first term of the right-hand side of (4.2) of [36], which does not appear in our formulas, comes from the second-order expansion of the last term of our (46). It is a quantity of the order of αp^4 in the ChPT counting scheme. Such terms have been systematically neglected, lying beyond the order αp^2 which defines the order of magnitude of terms that enter in our numerical evaluations. Numerically, the abovementioned term is equal to 10^{-5}, which justifies its neglect. Concerning the remaining part of (4.2) of [36] and (4.8), they correspond to our formulae obtained in second order of perturbation theory (81)–(84). Also, [36] neglects, in numerical calculations, the interference term of vacuum polarization with strong interaction, represented by the quantity $2\delta^{(2)}_{{\rm hvpol},n0}$ $(= 0.004)$ above, the latter being smaller than the uncertainties coming from the electromagnetic radiative corrections. Finally, another numerical difference appears from the values utilized for the electromagnetic radiative corrections and isospin symmetry breaking effects. We have used the results provided by [88, 89], which give directly the relative corrections and relative uncertainties (our (70) and (71)). Reference [36], using another publication of one of the authors of the above references, evaluates the relative corrections with a two-step procedure (4.4), (4.5), (4.9), (4.10) of [36], which results in slightly different values. The two results are, however, compatible within the existing uncertainties. A more accurate evaluation of the electromagnetic low energy constants, for instance by means of specific models, would considerably reduce those uncertainties and at the same time would remove accompanying ambiguities in numerical evaluations of related quantities.

The decay width of the ground state and the energy splitting between the $2P$ and $2S$ states take the following forms in the presence of the $O(\alpha)$ corrections:

$$\Gamma_{10} = 8 p^*_{10} \mu^2 \alpha^3 \left(a_0^-\right)^2 \left(1 + 0.046 \pm 0.014\right), \tag{94}$$

$$\left(E_{21} - E_{20}\right) = \frac{1}{4} \mu^2 \alpha^3 \left(a_0^+ + a_0^-\right) \left(1 + 0.023 \pm 0.032\right) + 0.29\ ({\rm eV})\,. \tag{95}$$

These formulas allow one to extract from the experimental results on the decay width and the energy splitting the values of the strong interaction scattering lengths a_0^- and a_0^+. We observe that the uncertainties in the corrective terms are much smaller in the decay width than in the energy splitting. This means that the decay width measurement will give us a more precise value for the scattering length a_0^- than the measurement of the energy splitting for the combination $(a_0^+ + a_0^-)$. On the other hand, the latter quantity is sensitive, through its dependence on the low energy constants L_4 and L_6, to the Zweig rule violating effects [70], and therefore its precise knowledge is of crucial importance for the understanding of the chiral symmetry breaking mechanism and of the dynamical role of the strange quark [91–94]. A precise knowledge of a_0^-, which mainly depends on the low energy constant L_5 [72], allows us to have a better insight into the ratio F_K/F_π of the kaon and pion weak decay constants [70].

Acknowledgements. One of us (H.S.) thanks L. Nemenov for stimulating discussions on hadronic atoms and informations on future projects about πK atoms, and B. Moussallam for discussions on πK scattering amplitudes. Feynman diagrams have been drawn with the package Axodraw: J.A.M. Vermaseren, Comp. Phys. Comm. 83 (1994) 45. This work was supported in part by the European Union network EURIDICE under EU RTN Contract CT2002-0311.

Appendix: Three- and four-dimensional integrals

Integrals are calculated with dimensional regularization, with dimension d close to 4. $\overline{\mu}$ is the mass scale of the d-dimensional theory.

For the various integrals with two, three or four propagators, we use a notation similar to that of Brown and Feynman [95]. In an elastic two-particle scattering process, we designate by p_1 and p_2 the incoming particle momenta, with masses m_1 and m_2, respectively, and by p'_1 and p'_2

the outgoing particle momenta, with the total momentum $P=(p_1+p_2)=(p_1'+p_2')$ and the momentum transfer $q=(p_1-p_1')=(p_2'-p_2)$; the Mandelstam variables are: $s=P^2$, $t=q^2$, $u=(p_1-p_2')^2$.

For the propagators, we use simplified notations, where k is the loop momentum variable:

$$\begin{aligned}
\frac{1}{(1)}&=\frac{\mathrm{i}}{(p_1-k)^2-m_1^2+\mathrm{i}\varepsilon}\,,\ \frac{1}{(2)}=\frac{\mathrm{i}}{(p_2+k)^2-m_2^2+\mathrm{i}\varepsilon}\,,\\
\frac{1}{(-1')}&=\frac{\mathrm{i}}{(-p_1'-k)^2-m_1^2+i\varepsilon}\,,\\
\frac{1}{(-2')}&=\frac{\mathrm{i}}{(-p_2'+k)^2-m_2^2+i\varepsilon}\,,\\
\frac{1}{(0)}&=\frac{-\mathrm{i}}{k^2+\mathrm{i}\varepsilon}\,,\quad \frac{1}{(3)}=\frac{-\mathrm{i}}{(q-k)^2+\mathrm{i}\varepsilon}\,.
\end{aligned}\tag{A.1}$$

The definitions of the integrals are:

$$\begin{aligned}
J&=\int[\mathrm{d}k]\,\frac{1}{(1)(2)(0)(3)}\,,\quad F=\int[\mathrm{d}k]\,\frac{1}{(1)(2)(3)}\,,\\
H&=\int[\mathrm{d}k]\,\frac{1}{(1)(2)(0)}\,,\quad G^{(1)}=\int[\mathrm{d}k]\,\frac{1}{(1)(0)(3)}\,,\\
G^{(2)}&=\int[\mathrm{d}k]\,\frac{1}{(2)(0)(3)}\,,\quad A=\int[\mathrm{d}k]\,\frac{1}{(1)(2)}\,,
\end{aligned}\tag{A.2}$$

where $[\mathrm{d}k]=\overline{\mu}^{4-d}\mathrm{d}^{\mathrm{d}}k/(2\pi)^d$. Vector and tensor generalizations of these integrals correspond to the cases where momenta k_μ or $k_\mu k_\nu$ appear in the numerator of the integrands.

Crossed diagrams involve integrals where (2) is replaced by $(-2')$. The corresponding integrals are defined as:

$$J(1,-2')=\int[\mathrm{d}k]\,\frac{1}{(1)(-2')(0)(3)}\,,\tag{A.3}$$

etc.

Constraint diagrams involve three-dimensional integrals which result from the s-channel four-dimensional integrals by the replacement of the two propagators of the incoming particles by the single effective propagator g_0 [see (5)]. The corresponding integrals are in the c.m. frame

$$\begin{aligned}
J^C&=-\frac{2\pi}{2\sqrt{s}}\int[\mathrm{d}k]\,\delta(k_0)\,\frac{1}{(1)(0)(3)}\,,\\
F^C&=-\frac{2\pi}{2\sqrt{s}}\int[\mathrm{d}k]\,\delta(k_0)\,\frac{1}{(1)(3)}\,,\\
H^C&=-\frac{2\pi}{2\sqrt{s}}\int[\mathrm{d}k]\,\delta(k_0)\,\frac{1}{(1)(0)}\,,\\
A^C&=-\frac{2\pi}{2\sqrt{s}}\int[\mathrm{d}k]\,\delta(k_0)\,\frac{1}{(1)}\,.
\end{aligned}\tag{A.4}$$

The factor $1/(2\sqrt{s})$ that has been incorporated in the definitions takes account of the fact that constraint diagrams contain one more scattering amplitude than the four-dimensional integrals and the latter is defined with the factor $\mathrm{i}/(2\sqrt{s})$ [see (2)]; the factor i is now contained in the definition of the meson propagator; the minus sign is reminiscent of a similar sign in front of g_0 in (3).

The three-dimensional integral of the effective propagator g_0 [see (4)–(5)] is, in the vicinity of $d=4$:

$$\begin{aligned}
i2\sqrt{s}\,A^C&=\overline{\mu}^{4-d}\int\frac{\mathrm{d}^{d-1}k}{(2\pi)^{d-1}}\,\frac{1}{b_0^2(s)-\mathbf{k}^2+\mathrm{i}\varepsilon}\\
&=\frac{1}{4\pi}\sqrt{-b_0^2(s)}\left[1+\left(\frac{d}{2}-2\right)\right.\\
&\quad\left.\times\left(-\psi(1)-2+\ln\left(\frac{-4b_0^2(s)}{4\pi\overline{\mu}^2}\right)\right)\right],
\end{aligned}\tag{A.5}$$

where $-b_0^2(s)$ is taken positive and ψ is the logarithmic derivative of the Gamma function. Analytic continuation to positive values of $b_0^2(s)$ is done with the replacement $\sqrt{-b_0^2(s)}\to-\mathrm{i}\sqrt{b_0^2}(s)$.

The integral A is

$$\begin{aligned}
A=\frac{\mathrm{i}}{16\pi^2}&\left[\frac{2}{d-4}-\psi(1)-2+\ln\left(\frac{m_1m_2}{4\pi\overline{\mu}^2}\right)\right.\\
&\left.+\frac{\left(m_1^2-m_2^2\right)}{2s}\ln\left(\frac{m_1^2}{m_2^2}\right)+Q(s)\right],
\end{aligned}\tag{A.6}$$

with

$$Q(s)=\begin{cases}
+\frac{\sqrt{4sb_0^2(s)}}{s}\left[\ln\left(\frac{\sqrt{s-(m_1-m_2)^2}+\sqrt{s-(m_1+m_2)^2}}{\sqrt{s-(m_1-m_2)^2}-\sqrt{s-(m_1+m_2)^2}}\right)-\mathrm{i}\pi\right],\\
(m_1+m_2)^2<s,\\
+\frac{\sqrt{-4sb_0^2(s)}}{s}\left[\pi-\arctan\left(\frac{\sqrt{-4sb_0^2(s)}}{s-(m_1^2+m_2^2)}\right)\right],\\
(m_1-m_2)^2<s<(m_1+m_2)^2,\\
-\frac{\sqrt{4sb_0^2(s)}}{s}\ln\left(\frac{\sqrt{(m_1+m_2)^2-s}+\sqrt{(m_1-m_2)^2-s}}{\sqrt{(m_1+m_2)^2-s}-\sqrt{(m_1-m_2)^2-s}}\right),\\
s<(m_1-m_2)^2.
\end{cases}\tag{A.7}$$

The integral of $\widetilde{G}_0$, entering in (6), (65) and (74), is equal to $-\mathrm{i}2\sqrt{s}A$.

The integral J is equal, on the mass shell, to

$$\begin{aligned}
J=-\frac{\mathrm{i}}{16\pi^2}&\frac{1}{t\sqrt{-b_0^2(s)s}}\left[\frac{2}{d-4}-\psi(1)+\ln\left(\frac{-t}{4\pi\overline{\mu}^2}\right)\right]\\
&\times\left[\arctan\left(\frac{s+m_1^2-m_2^2}{2\sqrt{-b_0^2(s)s}}\right)+\arctan\left(\frac{s-m_1^2+m_2^2}{2\sqrt{-b_0^2(s)s}}\right)\right].
\end{aligned}\tag{A.8}$$

Its threshold expansion is obtained by taking into account the facts that $|t|\ll s\simeq(m_1+m_2)^2$, $|b_0^2(s)|\ll s$:

$$\begin{aligned}
J=-\frac{\mathrm{i}}{16\pi^2}&\frac{1}{t}\left[\frac{2}{d-4}-\psi(1)+\ln\left(\frac{-t}{4\pi\overline{\mu}^2}\right)\right]\\
&\times\left[\frac{\pi}{\sqrt{-b_0^2(s)s}}-\frac{1}{m_1m_2}\right]+O\left(\alpha^3\ln\alpha^{-1}\right)\,,
\end{aligned}\tag{A.9}$$

where the order of magnitudes are evaluated with the counting rules of the QED bound states. The latter expansion can also be obtained with the threshold expansion

method of [66]. The singularity in $1/\sqrt{-b_0^2(s)s}$ is produced by the potential momenta, while the term in $1/(m_1m_2)$ is produced by the soft momenta. Ultrasoft momenta do not contribute at leading orders, while the hard momenta contribute at $O(\alpha^3)$.

The expression of $J(1,-2')$ is obtained from that of J by the replacement of the variable s by u. Its threshold expansion is obtained by noticing that $u \simeq (m_1-m_2)^2 - t - b_0^2(s)(m_1+m_2)^2/(m_1m_2)$:

$$J(1,-2') = -\frac{\mathrm{i}}{16\pi^2}\frac{1}{t}\left[\frac{2}{d-4} - \psi(1) + \ln\left(\frac{-t}{4\pi\overline{\mu}^2}\right)\right]\frac{1}{m_1m_2} + O(\alpha^3\ln\alpha^{-1})\,. \tag{A.10}$$

The potential momenta do not contribute at leading order to $J(1,-2')$ and the leading term comes now from the soft momenta.

The three-dimensional integral J^C is equal to:

$$J^C = \frac{\mathrm{i}}{16\pi^2}\frac{1}{t}\left[\frac{2}{d-4} - \psi(1) + \ln\left(\frac{-t}{4\pi\overline{\mu}^2}\right)\right]\frac{\pi}{\sqrt{-b_0^2(s)s}}. \tag{A.11}$$

Taking now the sum of the integrals J, $J(1,-2')$ and J^C, we find that J^C cancels the potential momenta contribution of J, while the soft momenta contributions of J and $J(1,-2')$ cancel each other:

$$J + J(1,-2') + J^C = O(\alpha^3\ln\alpha^{-1})\,. \tag{A.12}$$

A similar type of analysis also applies to the sum of the three diagrams (b)–(d) of Fig. 2 arising in QED. Here, the couplings being vector-like, one first decomposes the various integrals into a tensor sum, involving integrals of the types J, F, H, G, etc. and their vector and tensor associates. Taking into account the α^2 factor coming from the couplings, the sum of all these contributions vanishes up to order α^4. (Notice that the constraint diagrams should be calculated as three-dimensional integrals involving g_0 and one or two on-mass shell one-photon exchange diagrams.)

The above result does not remain true in an off-mass shell formalism. Here, the scattering amplitude is no longer gauge invariant and slight differences arise. The sum (A.12) yields now a $O(\alpha)$ term and generally the sum of the three previous diagrams behaves as $O(\alpha^3)$ [48]. The latter term, which is spurious, is cancelled by a higher-order diagram. Nevertheless, in the Fried–Yennie gauge [51], the same results as in the on-mass shell formalism occur.

Integrals F and H appear also in electromagnetic radiative corrections to the strong interaction. Integral H appears in diagram (c) of Fig. 4; diagram (b) corresponds to its crossed diagram involving $H(1,-2')$; diagram (d) involves H^C; diagram (a) involves H in the t-channel. H has the following threshold expansion:

$$\begin{aligned} H = {} & -\frac{1}{32\pi^2}\frac{\pi}{\sqrt{-b_0^2(s)s}}\left[\frac{2}{d-4} - \psi(1) + \ln\left(\frac{-4b_0^2(s)}{4\pi\overline{\mu}^2}\right)\right] \\ & -\frac{1}{32\pi^2 s}\left\{\left[\frac{2}{d-4} - \psi(1) + \ln\left(\frac{s}{4\pi\overline{\mu}^2}\right) + 2\right]\frac{1}{\beta_1\beta_2}\right. \\ & \left. -2\left[\frac{1}{\beta_1}\ln\left(\frac{1}{\beta_1}\right) + \frac{1}{\beta_2}\ln\left(\frac{1}{\beta_2}\right)\right]\right\} + O(\alpha^4\ln\alpha^{-1})\,, \\ & \beta_1 = \frac{1}{2}\left(1 + \frac{m_1^2-m_2^2}{s}\right),\ \beta_2 = \frac{1}{2}\left(1 - \frac{m_1^2-m_2^2}{s}\right), \end{aligned} \tag{A.13}$$

where the dominant singularity comes from the potential momenta and the next-to-leading terms from the hard momenta. (The soft and ultrasoft momenta do not contribute at leading orders.)

The crossed integral to H is:

$$\begin{aligned} & H(1,-2') \\ & = \frac{1}{32\pi^2 s}\left\{\left[\frac{2}{d-4} - \psi(1) + \ln\left(\frac{s}{4\pi\overline{\mu}^2}\right) + 2\right]\frac{1}{\beta_1\beta_2}\right. \\ & \quad \left. + \frac{2}{(\beta_1-\beta_2)}\left[\frac{1}{\beta_1}\ln\left(\frac{1}{\beta_1}\right) - \frac{1}{\beta_2}\ln\left(\frac{1}{\beta_2}\right)\right]\right\} \\ & \quad + O(\alpha^4\ln\alpha^{-1})\,, \end{aligned} \tag{A.14}$$

where only hard momenta contribute. The integral entering in the t-channel vertex function (diagram (a) of Fig. 4) is $H(1,-1';m_1,m_1)$:

$$H(1,-1') = \frac{1}{32\pi^2 m_1^2}\left[\frac{2}{d-4} - \psi(1) + \ln\left(\frac{m_1^2}{4\pi\overline{\mu}^2}\right)\right] + O(\alpha^4\ln\alpha^{-1})\,. \tag{A.15}$$

It can also be obtained from the result (A.14), by taking in it the limit $m_2 \to m_1$.

H^C is equal to the opposite of the contribution of the potential momenta in H:

$$H^C = \frac{1}{32\pi^2}\frac{\pi}{\sqrt{-b_0^2(s)s}}\left[\frac{2}{d-4} - \psi(1) + \ln\left(\frac{-4b_0^2(s)}{4\pi\overline{\mu}^2}\right)\right]. \tag{A.16}$$

If $\Sigma(p^2,m^2)$ is the meson electromagnetic self-energy, taken for the moment with scalar couplings, then, after a mass-shell renormalization, it is the quantity $\frac{1}{2}\frac{\partial\Sigma}{\partial m^2}|_{p^2=m^2}$ that multiplies in lowest order the strong interaction vertex. This yields $-1/2$ of the value of the t-channel form factor at $t=0$ [see (A.15)]. The self-energy contributions of the two external mesons of that form factor then cancel the latter completely at leading order. Similarly, the sum of H, $H(1,-2')$ and H^C yields a finite $O(\alpha^3)$ term.

The above results should be completed by incorporating the vector coupling of the photon. The latter does not change the leading behavior of H^C. Concerning the four-dimensional integrals, the only modifications are through the hard momenta contributing with finite $O(\alpha^3)$ effects. (Loop momenta in the numerators improve the infrared behavior of the object.) Taking also into account the factor α coming from the photon couplings, the sum of all contributions reduces to a finite $O(\alpha^4)$ term.

Diagrams where the photon is emitted from the vertex are not infrared singular and give contributions of order α^4.

In the case of the charged–neutral channel (process $\pi^-K^+ \to \pi^0K^0$), the integrals of the t-channel and u-

channel form factors are absent. In that case, the cancellations occur between the sum $H + H^C$ and the contributions of the self-energies of the two external charged mesons, taking into account the vector coupling of the photon. The result is again a finite $O(\alpha^4)$ term.

The integral that contributes to the dominant part of the constraint diagram (d) of Fig. 5 is denoted I^{CC}; it is:

$$I^{CC} = \frac{1}{2\sqrt{s}}\,\overline{\mu}^{2(4-d)} \int \frac{\mathrm{d}^{d-1}k}{(2\pi)^{d-1}} \frac{\mathrm{d}^{d-1}k'}{(2\pi)^{d-1}} \frac{\mathrm{i}}{b_0^2(s) - \mathbf{k}^2 + \mathrm{i}\varepsilon} \times \frac{\mathrm{i}}{b_0^2(s) - \mathbf{k}'^2 + \mathrm{i}\varepsilon} \frac{(-\mathrm{i})}{-(\mathbf{k}-\mathbf{k}')^2 + \mathrm{i}\varepsilon} = \frac{\mathrm{i}}{64\pi^2\sqrt{s}} \left(\frac{1}{d-4} - \psi(1) - 1 + \ln\left(\frac{-4b_0^2(s)}{4\pi\overline{\mu}^2} \right) \right). \tag{A.17}$$

The integral that contributes to the dominant part of diagram (b) of Fig. 5, denoted I^C is calculated in the following way. One first calculates the four-dimensional integral on the mass shell; the latter is then integrated three-dimensionnally, by extending eventually the domain of validity of the momentum transfer squared t. The four-dimensional integral on the mass shell is nothing but H (A.13). The latter is independent of t. Hence the three-dimensional integration reduces to that of ig_0, given by (A.5) times i. The result is therefore the product of the right-hand sides of (A.13) and (A.5), times i; since the integral of g_0 is of order $\sqrt{-b_0^2(s)}$, it is sufficient to retain the dominant singularity of H. One finds the opposite value of I^{CC} (A.17). Hence the sum of the three constraint diagrams of Fig. 5 is given by the opposite value of I^{CC}; the finite logarithmic part of it cancels a similar term in the diagram (a) of Fig. 5 [66]. As we emphasized in Sect. 7 and Sect. 8, the infinite part of I^{CC} is cancelled by a similar term present in second order of the perturbation theory expansion of the bound state energy. The finite part that has been retained in the right-hand side of (84), second term, corresponds to the contribution of the factor $-b_0^2(s)$ of the logarithm.

The integrals G (A.2) are infrared finite and receive contributions at leading order from potential and soft momenta with the ratio $(2)/(-1)$:

$$G^{(a)} = -\frac{1}{32m_a}\frac{1}{\sqrt{-t}} + O(\alpha^3 \ln \alpha^{-1}), \quad a = 1, 2\,. \tag{A.18}$$

References

1. S. Deser, M.L. Goldberger, K. Baumann W. Thirring, Phys. Rev. **96**, 774 (1954)
2. J.L. Uretsky, T.R. Palfrey Jr., Phys. Rev. **121**, 1798 (1961)
3. T.L. Trueman, Nucl. Phys. **26**, 57 (1961)
4. S.M. Bilen'kii, N.V. Hieu, L.L. Nemenov, F.G. Tkebuchava, Sov. J. Nucl. Phys. **10**, 469 (1969)
5. L.L. Nemenov, Sov. J. Nucl. Phys. **41**, 629 (1985)
6. L. Afanasyev, G. Colangelo, J. Schacher, eds., HadAtom05, Mini-Proceedings of the Workshop on Hadronic Atoms, Preprint hep-ph/0508193, and references therein
7. B. Adeva et al., J. Phys. G **30**, 1929 (2004) [hep-ex/0409053]
8. B. Adeva et al., Phys. Lett. B **619**, 50 (2005) [hep-ex/0504044]; other references at http://dirac.web.cern.ch/DIRAC/
9. G.V. Efimov, M.A. Ivanov, V.E. Lyobovitskii, Sov. J. Nucl. Phys. **44**, 296 (1986)
10. A.A. Bel'kov, V.N. Pervushin, F.G. Tkebuchava, Sov. J. Nucl. Phys. **44**, 300 (1986)
11. U. Moor, G. Rasche, W.S. Woolcock, Nucl. Phys. A **587**, 747 (1995)
12. A. Gashi, G. Rasche, G.C. Oades, W.S. Woolcock, Nucl. Phys. A **628**, 101 (1998) [nucl-th/9704017]
13. A. Gashi, G.C. Oades, G. Rasche, W.S. Woolcock, Nucl. Phys. A **699**, 732 (2002) [hep-ph/0108116]
14. Z.K. Silagadze, JETP Lett. **60**, 689 (1994)
15. E.A. Kuraev, Phys. Atom. Nucl. **61**, 239 (1998) [hep-ph/9701237]
16. U. Jentschura, G. Soff, V. Ivanov, S.G. Karshenboim, Phys. Lett. A **241**, 351 (1998)
17. V. Lyubovitskij, A. Rusetsky, Phys. Lett. B **389**, 181 (1996) [hep-ph/9610217]
18. V.E. Lyubovitskij, E.Z. Lipartia, A.G. Rusetsky, JETP Lett. **66**, 783 (1997) [hep-ph/9801215]
19. M.A. Ivanov, V.E. Lyubovitskij, E.Z. Lipartia, A.G. Rusetsky, Phys. Rev. D **58**, 094024 (1998) [hep-ph/9805356]
20. H. Jallouli, H. Sazdjian, Phys. Rev. D **58**, 014011 (1998) [hep-ph/9706450]
21. H. Jallouli, H. Sazdjian, Phys. Rev. D **58**, 099901(E) (1998)
22. H. Sazdjian, in Proc. International Workshop Hadronic Atoms and Positronium in the Standard Model, ed. by M.A. Ivanov et al. (Dubna 1998), p. 50 [hep-ph/9809425]
23. H. Sazdjian, Phys. Lett. B **490**, 203 (2000) [hep-ph/0004226]
24. P. Labelle, K. Buckley, preprint hep-ph/9804201
25. X. Kong, F. Ravndal, Phys. Rev. D **59**, 014031 (1999) [hep-ph/9805357]
26. X. Kong, F. Ravndal, Phys. Rev. D **61**, 077506 (2000) [hep-ph/9905539]
27. B. Holstein, Phys. Rev. D **60**, 114030 (1999) [nucl-th/9901041]
28. A. Gall, J. Gasser, V.E. Lyubovitskij, A. Rusetsky, Phys. Lett. B **462**, 335 (1999) [hep-ph/9905309]
29. V. Antonelli, A. Gall, J. Gasser, A. Rusetsky, Ann. Phys. (New York) **286**, 108 (2001) [hep-ph/0003118]
30. J. Gasser, V.E. Lyubovitskij, A. Rusetsky, A. Gall, Phys. Rev. D **64**, 016008 (2001) [hep-ph/0103157]
31. D. Eiras, J. Soto, Phys. Rev. D **61**, 114027 (2000) [hep-ph/9905543]
32. D. Eiras, J. Soto, Phys. Lett. B **491**, 101 (2000) [hep-ph/0005066]
33. B. Adeva et al., CERN-SPSC-2004-009, at http://dirac.web.cern.ch/DIRAC/future.html
34. Letters of intent for GSI and J-PARC at http://dirac.web.cern.ch/DIRAC/
35. J. Schweizer, Phys. Lett. B **587**, 33 (2004) [hep-ph/0401048]
36. J. Schweizer, Eur. Phys. J. C **36**, 483 (2004) [hep-ph/0405034]

37. W.E. Caswell, G.P. Lepage, Phys. Lett. B **167**, 437 (1986)
38. A.A. Logunov, A.N. Tavkhelidze, Nuovo Cim. **29**, 380 (1963)
39. R. Blankenbecler, R. Sugar, Phys. Rev. **142**, 1051 (1966)
40. F. Gross, Phys. Rev. **186**, 1448 (1969)
41. M.H. Partovi, E.L. Lomon, Phys. Rev. D **2**, 1999 (1970)
42. C. Fronsdal, R.W. Huff, Phys. Rev. D **3**, 933 (1971)
43. V.B. Mandelzweig, S.J. Wallace, Phys. Lett. B **197**, 469 (1987)
44. R.N. Faustov, Theor. Math. Phys. **3**, 478 (1970)
45. I.T. Todorov, Phys. Rev. D **3**, 2351 (1971)
46. I.T. Todorov, in: Properties of Fundamental Interactions, ed. by A. Zichichi, (Editrice Compositori, Bologna, 1973), Vol. 9, Part C, p. 951
47. G.P. Lepage, Phys. Rev. A **16**, 863 (1977)
48. H. Jallouli, H. Sazdjian, Ann. Phys. (New York) **253**, 376 (1997) [hep-ph/9602241]
49. H.A. Bethe, Phys. Rev. **72**, 339 (1947)
50. H.A. Bethe, L.M. Brown, J.R. Stehn, Phys. Rev. **77**, 370 (1950)
51. H.M. Fried, D.R. Yennie, Phys. Rev. **112**, 1391 (1958)
52. P.A.M. Dirac, Lectures on Quantum Mechanics, Belfer Graduate School of Science Monograph Series (Yeshiva University, New York, 1964)
53. E.C.G. Sudarshan, N. Mukunda, Classical Dynamics: A Modern perspective (Wiley, New York, 1974)
54. A.J. Hanson, T. Regge, C. Teitlboim, Constraint Hamiltonian Systems, Contributi del Centro Linceo Interdisciplinare di Scienze Matematiche Fisiche e loro Applicazioni 22 (Academia Nazionale del Lincei, Roma, 1976)
55. K. Sundermeyer, Constrained Dynamics, Lecture Notes in Physics (Springer, Berlin, 1982), Vol. 169
56. P. Droz-Vincent, Lett. Nuovo Cimento **1**, 839 (1969)
57. T. Takabayasi, Prog. Theor. Phys. **54**, 563 (1975)
58. I.T. Todorov, Dubna Report No. E2-10125, 1976 (unpublished)
59. A. Komar, Phys. Rev. D **18**, 1881 (1978)
60. H. Leutwyler, J. Stern, Phys. Lett. B **73**, 75 (1978)
61. H.W. Crater, P. Van Alstine, Ann. Phys. (New York) **148**, 57 (1983)
62. H. Sazdjian, Phys. Rev. D **33**, 3401 (1986)
63. A.N. Mitra, I. Santhanam, Few-body Syst. **12**, 41 (1992)
64. G. Longhi, L. Lusanna, eds., Constraint's Theory and Relativistic Dynamics, Proc. Firenze Workshop (World Scientific, Singapore, 1987)
65. G.T. Bodwin, D.R. Yennie, Phys. Rep. **43**, 267 (1978)
66. M. Beneke, V.A. Smirnov, Nucl. Phys. B **552**, 321 (1998) [hep-ph/9711391]
67. J. Schwinger, J. Math. Phys. **5**, 1606 (1964)
68. S. Weinberg, Physica A **96**, 327 (1979)
69. J. Gasser, H. Leutwyler, Ann. Phys. (New York) **158**, 142 (1984)
70. J. Gasser, H. Leutwyler, Nucl. Phys. B **250**, 465 (1985)
71. S. Weinberg, Phys. Rev. Lett. **17**, 616 (1966)
72. V. Bernard, N. Kaiser, U.-G. Meissner, Nucl. Phys. B **357**, 129 (1991)
73. J. Bijnens, P. Dhonte, P. Talavera, J. High Energ. Phys. **0405**, 036 (2004) [hep-ph/0404150]
74. S.M. Roy, Phys. Lett. B **36**, 353 (1971)
75. F. Steiner, Fortschr. Phys. **19**, 115 (1971)
76. P. Büttiker, S. Descotes-Genon, B. Moussallam, Eur. Phys. J. C **33**, 409 (2004) [hep-ph/0310283]
77. J. Schweizer, Phys. Lett. B **625**, 217 (2005) [hep-ph/0507323]
78. R. Kaiser, J. Schweizer, J. High Energ. Phys. **0606**, 009 (2006) [hep-ph/0603153]
79. K. Kampf, B. Moussallam, Eur. Phys. J. C **47**, 723 (2006) [hep-ph/0604125]
80. A. Nandy, Phys. Rev. D **5**, 1531 (1972)
81. E.M. Lifshitz, L.P. Pitaevskii, Relativistic Quantum Theory (Pergamon Press, Oxford, 1974), p. 421
82. J. Bijnens, P. Talavera, J. High Energ. Phys. **0203**, 046 (2002) [hep-ph/0203049]
83. R. Urech, Nucl. Phys. B **433**, 234 (1995) [hep-ph/9405341]
84. M. Knecht, R. Urech, Nucl. Phys. B **519**, 328 (1998) [hep-ph/9709348]
85. V.E. Lyubovitskij, A.G. Rusetsky, Phys. Lett. B **494**, 9 (2000) [hep-ph/0009206]
86. A. Nehme, P. Talavera, Phys. Rev. D **65**, 054023 (2002) [hep-ph/0107299]
87. A. Nehme, Eur. Phys. J. C **23**, 707 (2002) [hep-ph/0111212]
88. B. Kubis, U.-G. Meissner, Nucl. Phys. A **699**, 709 (2002) [hep-ph/0107199]
89. B. Kubis, Phys. Lett. B **529**, 69 (2002) [hep-ph/0112154]
90. W.E. Caswell, G.P. Lepage, Phys. Rev. A **18**, 810 (1978)
91. B. Moussallam, Eur. Phys. J. C **14**, 111 (2000) [hep-ph/9909292]
92. B. Moussallam, J. High Energ. Phys. **0008**, 005 (2000) [hep-ph/0005245]
93. S. Descotes, L. Girlanda, J. Stern, J. High Energ. Phys. **0001**, 041 (2000) [hep-ph/9910537]
94. S. Descotes-Genon, J. Stern, Phys. Lett. B **488**, 274 (2000) [hep-ph/0007082]
95. L.M. Brown, R.P. Feynman, Phys. Rev. **85**, 231 (1952)